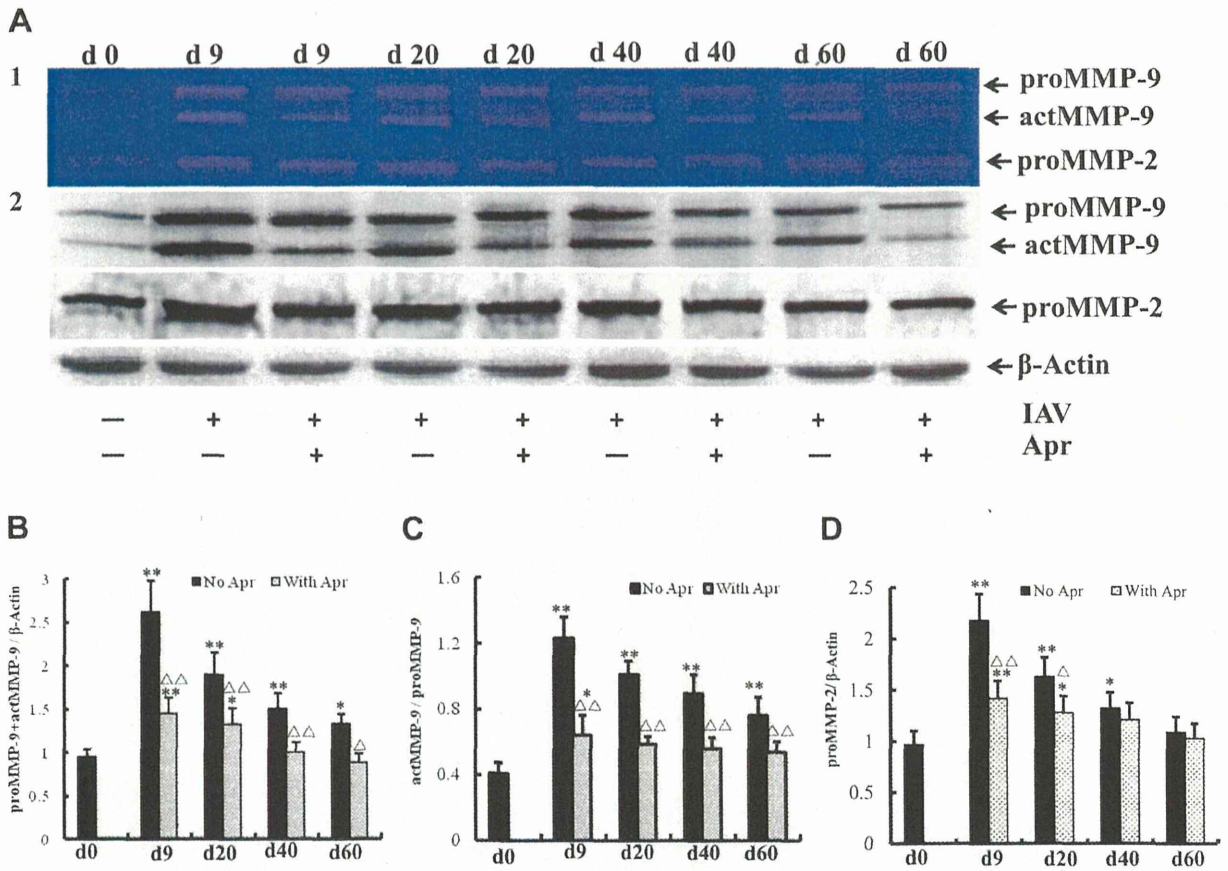

Fig. 3. Upregulation and activation of pro-matrix metalloproteinases (pro-MMPs) in the myocardium and effects of trypsin inhibitor. *A*: kinetics of activity and upregulation of MMPs in hearts as determined by zymography (*1*) and Western blot analysis (*2*) from *days 0* to *60* postinfection. β-Actin was the internal control. *B–D*: densitometry showed significant inhibition of upregulation of pro-MMP9 + active (act)MMP9 (*B*), pro-MMP-2 (*C*), and activation of pro-MMP-9 (*D*) by Apr after IAV infection. Data are averages ± SD of 3 independent experiments from 7–10 mice/group. $^{*}P < 0.05$ and $^{**}P < 0.01$ vs. *day 0*; $\triangle P < 0.05$ and $\triangle\triangle P < 0.01$ vs. no Apr treatment at the same time after IAV infection.

degradation, collagen deposition, and Col I and Col III mRNA in the myocardium increased in IAV-induced acute and chronic myocarditis. The differential increase in Col I and Col III mRNA led to a decreased Col I-to-Col III ratio. Fourth, cardiac function was transiently impaired in the acute stage and deteriorated with progressive ventricular dilation during the chronic stage. Finally, trypsin inhibitor aprotinin suppressed pro-MMP-9 activation and cytokine release, alleviated myocardial inflammation, reduced collagen proliferation, and restored collagen metabolism, thus effectively preventing ventricular dilation and DCM for improved cardiac function.

Consistent with our previous study (39), we found that IAV infection significantly upregulated ectopic trypsin, pro-MMPs, and proinflammatory cytokines in acute myocarditis. However, by *day 20* postinfection, although replication of IAV could not be detected in the myocardium, upregulation of trypsin, MMPs, and proinflammatory cytokines persisted during the chronic stage. One possible reason for the persistent upregulation of these factors might be a trypsin-MMP-9-cytokine cycle in the myocardium. Initially, IAV infection induces upregulation of trypsinogen, pro-MMPs, and proinflammatory cytokines through the Toll-like receptor 7/8-myeloid differentiation primary response protein 88-NF-κB/activator protein (AP)-1 signaling pathway in the acute stage (40, 50). Induced trypsinogen is converted to trypsin through autoactivation or by widely distributed endogenous activators (13). Trypsin converts upregulated pro-MMP-9 to active MMP-9 and promotes proinflammatory cytokine secretion through PAR-2 (35, 39, 44). MMP-9 activates proinflammatory cytokines such as IL-6, IL-1β, and TNF-α to active forms (9, 42), which, in turn, promote transcription of trypsinogen and pro-MMPs (50, 51). In this model, the interrelationship of trypsin, MMP-9, and cytokines is a cycle that contributes to persistent upregulation of these factors even after IAV is no longer present in the myocardium. Another reason for the persistent upregulation of these factors might be the effects of inflammatory cells infiltrating the myocardial interstitium. These cells release IL-1β, IL-6, and TNF-α, which enhance the transcription of trypsin and MMPs genes via NF-κB and AP-1 (39, 51). Trypsin and MMP-9 synergistically promote inflammatory cell migration across the ECM to inflammatory loci (39, 53). These migrating cells further induce upregulation of trypsin and MMPs by releasing cytokines in inflammatory loci, leading to persistent upregulation. The colocalization of upregulated trypsin and inflammatory infiltrates we observed during acute and chronic stages suggests a close relationship among these pathogenic factors that results in chronic myocardial inflammation.

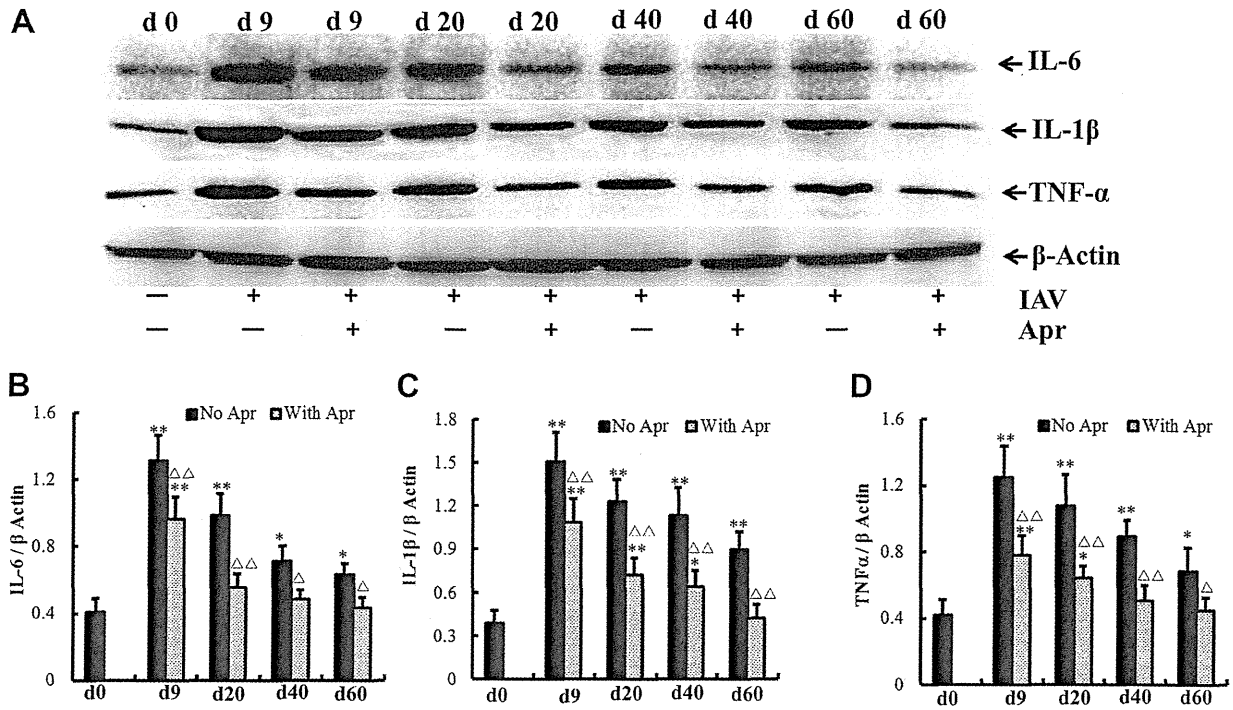

Fig. 4. Cytokine induction in the myocardium and suppression by trypsin inhibitor. *A*: time courses of induction of IL-6, IL-1β, and TNF-α from *days 0* to *60* postinfection by Western blot analysis. β-Actin was the internal control. *B–D*: densitometry showed that Apr significantly inhibited the induction of IL-6 (*B*), IL-1β (*C*), and TNF-α (*D*) during acute and chronic phases of myocarditis. Data are means ± SD of 3 independent experiments from 7–10 mice/group. $^{*}P < 0.05$ and $^{**}P < 0.01$ vs. *day 0*; $^{\triangle}P < 0.05$ and $^{\triangle\triangle}P < 0.01$ vs. no Apr at the same time after IAV infection.

Although IAV replication, myocardial inflammation, and expression of MMPs, trypsin, and proinflammatory cytokines were significantly inhibited by *day 9* postinfection in mice treated with aprotinin, the pathological changes in the myocardium persisted without recovery until after 40–60 days of continuous treatment with aprotinin. These findings suggested that trypsin might be involved in the pathological process throughout acute and chronic phases of myocarditis after IAV infection.

In the trypsin-MMP-9-cytokine cycle, the regulation of trypsin expression is crucial for cycle maintenance. In the acute stage, trypsin was significantly upregulated by IAV infection and peaked on *day 9* postinfection. Induced trypsin activates PAR-2 to evoke cytokine release, which, in turn, upregulates trypsin expression through activation of NF-κB and AP-1 (40, 50). However, PAR-2 is the "sensory" arm of a negative feedback mechanism to downregulate trypsin expression (25). Activated PAR-2 forms a complex with β-arrestin and ERK1/2, which effectively prevents ERK1/2 translocation into the nucleus and after transcription of trypsinogen (6, 47). Trypsin expression gradually declined from *day 20* postinfection accompanied by the clearance of IAV. The final level of trypsin depended on the balance between its up- and downregulation mechanisms.

In the present study, both pro-MMP-2 and pro-MMP-9 in the myocardium were upregulated during acute and chronic phases. However, only pro-MMP-9 was activated, probably because pro-MMP-2 is resistant to activation by trypsin (19). MMP-9 also cleaves Col I and Col III, whereas MMP-2 does not (36). Trypsin has three major isoforms. In cardiac tissue, $trypsin_2$ is the major isoform and its abundance is nearly double that of $trypsin_1$, whereas $trypsin_3$ is barely detectable (39). $Trypsin_2$ degrades Col I and is an efficient activator of a prourokinase cascade and procollagenases (33). Consistent with the kinetic expression of trypsin and MMP-9 that we observed in the myocardium, circulating ICTP, which reflects degradation of Col I, increased prominently in early stages and then slightly in late stages. In response to increased collagen degradation, the lost collagen was replaced by newly synthesized collagen, which was distributed around inflammatory loci in the acute phase and extensively proliferated across the ventricular interstitium in the chronic phase. Col I and Col III are the main components of the myocardial ECM. During collagen proliferation, Col I and Col III mRNA (especially Col III) was significantly increased. The differential increase of Col I and Col III mRNA led to a decreased Col I-to-Col III mRNA ratio in the myocardium. The increased ICTP and decreased relative proportion of Col I and Col III mRNA indicated that in ECM remodeling, properly cross-linked Col I was increasingly degraded and replaced with poorly cross-linked Col III. Col I provides substantial tensile and stiffness to prevent slippage and overstretching of myocytes, whereas Col III has greater elasticity (54). These changes might promote ventricular myocyte slippage and chamber dilation that contribute to wall thinning and systolic dysfunction in the development of DCM.

The reasons for the differential increase in Col I and Col III expression after IAV infection might be different molecular mechanisms. IL-6, IL-1β, and TNF-α were persistently upregulated during acute and chronic phases after IAV infection. Previous studies (10, 32) have indicated that IL-1β and IL-6

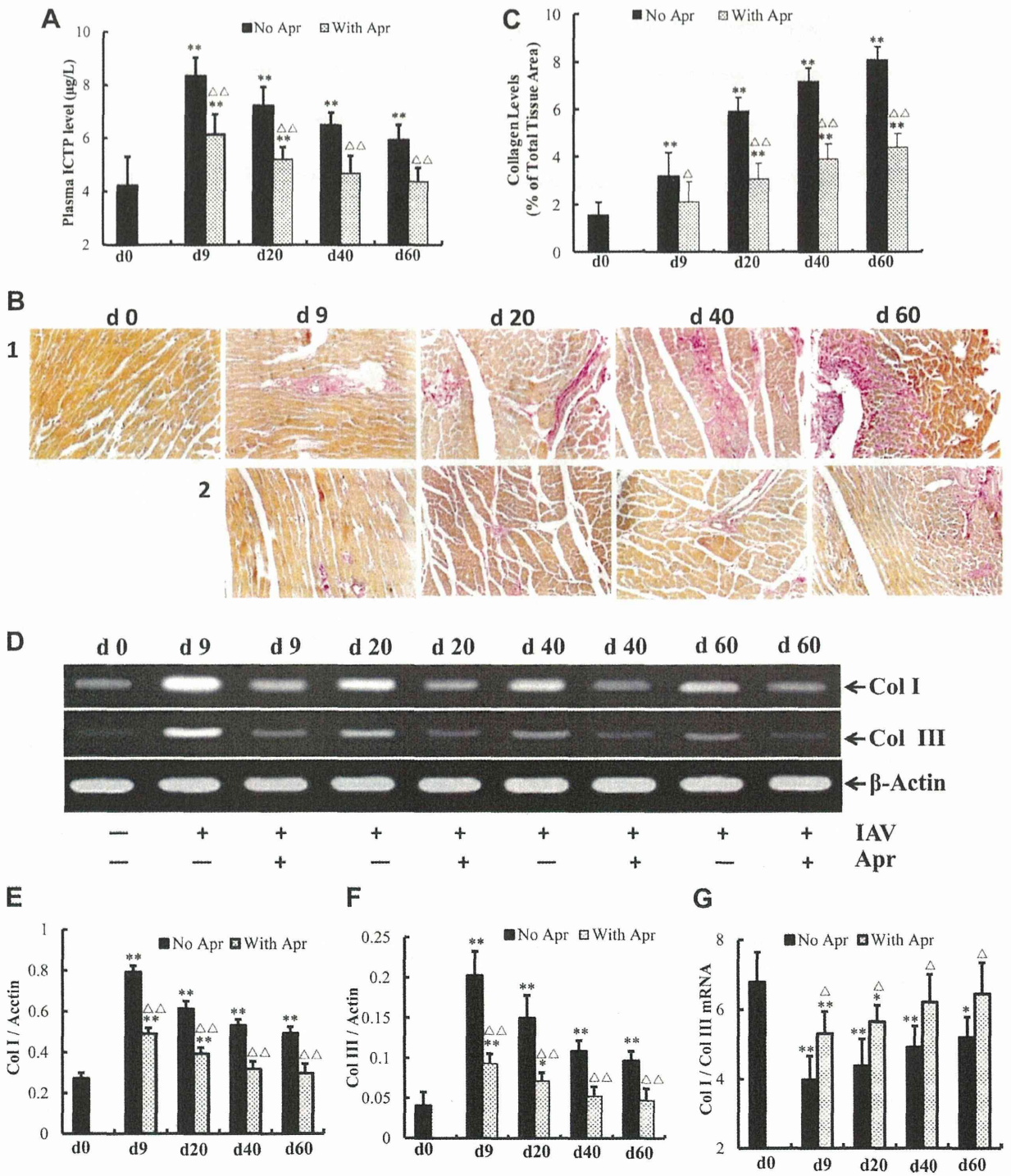

Fig. 5. Increased collagen type I (Col I) degradation, upregulation of collagen synthesis, and effect of trypsin inhibitor. *A*: Col I degradation as measured by plasma Col I cross-linked carboxy-terminal telopeptide (ICTP) during acute and chronic phases (n = 7–10 mice/group). Apr effectively prevented degradation.. *B*: proliferation of collagen in the myocardium as identified by van Gieson staining from *days 0* to *60* without (*1*) and with (*2*) Apr treatment. Magnification: ×100. *C*: quantification of collagen as percent area (n = 5 mice/group). *D*: synthesis of Col I and collagen type III (Col III) as assessed by Col I and Col III mRNA using RT-PCR. β-Actin was the internal control. *E–G*: densitometry showed significantly upregulated Col I (*E*) and Col III (*F*) mRNA and a decreased Col I-to-Col III mRNA ratio (*G*) in IAV-induced acute and chronic myocarditis. Data are means ± SD of 3 independent experiments from 7–10 mice/group. $^{*}P < 0.05$ and $^{**}P < 0.01$ vs. *day 0*; $\triangle P < 0.05$ and $\triangle\triangle P < 0.01$ vs. no Apr treatment at the same time point.

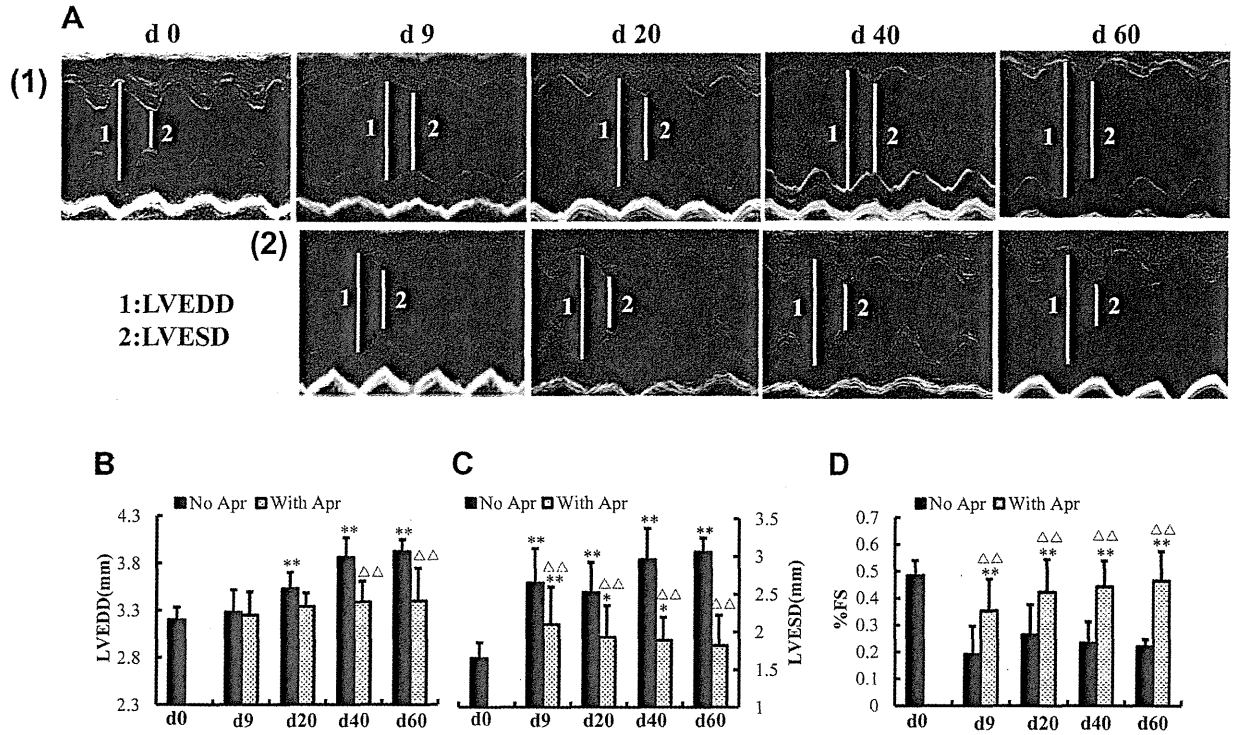

Fig. 6. Progressive left ventricular (LV) dilation and restoration by trypsin inhibitor. *A*: representative M-mode echocardiogram images of mice from *days 0* to *60* postinfection without (*1*) or with (2) Apr treatment. *B–D*: measurements of LV end-diastolic dimension (LVEDD; *B*), LV end-systolic dimension (LVESD; *C*), and fractional shortening (FS; in %; *D*) at the indicated time points showed inhibition of LV dilation and improvement of LV function with Apr after IAV infection. n = 7–10 mice/group. $^{*}P < 0.05$ and $^{**}P < 0.01$ vs. *day 0*; $\triangle\triangle P < 0.01$ vs. no Apr at the same time of observation.

induce collagen synthesis through upregulation of Col I and Col III genes. In contrast, TNF-α reduces Col I mRNA levels and the steady state of Col I mRNA but has no effect on Col III mRNA (30, 43). In our study, differential regulatory effects of cytokines on Col I and Col III mRNA might have resulted in the shift of the Col I-to-Col III mRNA ratio in the development of DCM after IAV infection.

Trypsin is an efficient activator of a prourokinase cascade (33). Plasminogen is the primary physiological substrate of urokinase. Plasminogen is activated in patients with acute viral myocarditis at all stages of the clinical course (7). Plasmin can directly degrade basement collagen type IV (27) and activate MMP-9 (12). The combined upregulation of trypsin and plasmin activity causes synergistic proteolytic degradation of the vascular basement and the myocardial ECM. In addition to trypsin, aprotinin also inhibits plasmin activity, thus effectively protecting the heart from inflammatory injury and myocardial remodeling.

No specific treatment is currently available for the prevention of IAV-induced myocarditis and subsequent DCM. Heymans et al. (12) reported that suppression of MMP-9 activity reduces the cardiac inflammatory response, protecting mice against cardiac injury, dilatation, and failure during viral myocarditis. However, Cheng et al. (3) indicated that MMP-9 is

Table 1. *Effects of the trypsin inhibitor Apr on kinetics of cardiac function and LV posterior wall thickness after influenza A virus infection*

	Day 0	*Day 9*		*Day 20*		*Day 40*		*Day 60*	
Parameters	Control	No Apr	With Apr	No Apr	With Apr	No Apr	With Apr	No Apr	With Apr
n	10	8	9	7	9	7	9	7	9
Ejection fraction, %	70.51 ± 9.06	49.94 ± 8.26†	60.36 ± 6.46*‡	52.35 ± 11.01†	61.89 ± 8.87*‡	49.28 ± 5.08†	63.27 ± 12.71§	47.67 ± 8.53†	65.05 ± 9.26§
Stroke volume, μl	44.56 ± 3.74	31.42 ± 3.43†	37.42 ± 4.34†§	31.82 ± 5.55†	38.25 ± 3.31†§	32.48 ± 3.97†	40.67 ± 6.09§	31.61 ± 4.36†	42.49 ± 4.90§
Cardiac output, ml/min	24.06 ± 3.63	18.22 ± 2.45†	21.55 ± 3.08*§	18.27 ± 2.60†	21.89 ± 2.01§	18.20 ± 2.50†	22.92 ± 2.75§	18.06 ± 3.32†	23.87 ± 2.47§
LV posterior wall thickness at end diastole, mm	0.74 ± 0.07	0.76 ± 0.08	0.75 ± 0.06	0.69 ± 0.08	0.73 ± 0.07	0.64 ± 0.07*	0.73 ± 0.06‡	0.61 ± 0.08†	0.71 ± 0.09‡
LV posterior wall thickness at end systole, mm	1.15 ± 0.07	1.17 ± 0.07	1.16 ± 0.06	1.13 ± 0.06	1.15 ± 0.07	1.03 ± 0.08†	1.14 ± 0.05§	0.98 ± 0.06†	1.14 ± 0.06§

Values are means ± SD; n, number of surviving mice. $^{*}P < 0.05$ and $^{\dagger}P < 0.01$ compared with *day 0*; $^{\ddagger}P < 0.05$ and $^{\S}P < 0.01$ compared with no aprotinin (Apr) treatment at the same time of observation.

essential for viral clearance by promoting immune cell recruitment in the early phase of infection. Therefore, MMP-9 inhibition might impair host defense and enhance infection dissemination. In our study, administration of the trypsin inhibitor aprotinin effectively suppressed IAV replication and the inflammatory response throughout acute and chronic phases by inhibiting trypsin-mediated activation of IAV hemagglutinin and interrupting the trypsin-MMP-9-cytokine cycle. Thus, inhibition of MMP-9 activity by aprotinin will not impair the host defense against viral infection. In addition, recent studies (2, 34, 52) have reported that PAR-2 is involved in innate immune responses during RNA virus infection and enhanced cardiac remodeling in the injured heart. Activation of PAR-2 negatively regulates the Toll-like receptor-3-dependent antiviral pathway with reduced expression of interferon-β (34). PAR-2 knockout mice are protected from H1N1/PR8 IAV virus-induced lethality and coxsackievirus B3-induced myocarditis (34, 52). Overexpression of PAR2 in mice induced cardiac fibrosis, inflammation, and heart failure (2). As trypsin is one of the most potent activators of PAR-2, aprotinin can partially abrogate the pathological roles of PAR-2 induced by trypsin.

Study limitations. Our findings suggested that trypsin is a key factor in acute and chronic stages of myocarditis after IAV infection. An experiment in which aprotinin treatment started from *day 9* postinfection could further confirm the protective effects of trypsin inhibitor during chronic stage but was not performed. Thus, we cannot exclude the contribution of reduced acute myocarditis by aprotinin treatment for the prevention of DCM.

Conclusions. The results of the present study suggested that ectopic trypsin in the myocardium was involved in acute and chronic myocardial inflammation by promoting IAV infection and initiating a trypsin-MMP-9-cytokine cycle and promotes progressive cardiac dilation through mediation of collagen remodeling. Thus, trypsin might play important roles in the development of DCM after IAV infection. Aprotinin prevented the progression of myocarditis to DCM by suppressing IAV infection, interrupting the trypsin-MMP-9-cytokine cycle and restoring collagen metabolism. Our findings suggest that inhibition of trypsin activity might be a promising therapeutic approach for the prevention of DCM after IAV infection.

ACKNOWLEDGMENTS

The authors are grateful to Dr. Le Gui for the excellent technical assistance.

GRANTS

Financial support for this work was provided by National Natural Science Funds of China Grant 81100154 and Summit of the Six Top Talents Program of Jiangsu Province Grant 2011-WS-059.

DISCLOSURES

No conflicts of interest, financial or otherwise, are declared by the author(s).

AUTHOR CONTRIBUTIONS

Author contributions: H.-Y.P., H.K., and J.-H.Z. conception and design of research; H.-Y.P., H.-M.S., and L.-J.X. performed experiments; H.-Y.P. and J.-H.Z. drafted manuscript; H.-Y.P., H.-M.S., L.-J.X., M.P., Y.-P.W., H.K., and J.-H.Z. approved final version of manuscript; M.P. and Y.-P.W. analyzed data.

REFERENCES

1. **Al-Amoodi M1, Rao K, Rao S, Brewer JH, Magalski A, Chhatriwalla AK.** Fulminant myocarditis due to H1N1 influenza. *Circ Heart Fail* 3: e7–e9, 2010.
2. **Antoniak S, Sparkenbaugh EM, Tencati M, Rojas M, Mackman N, Pawlinski R.** Protease activated receptor-2 contributes to heart failure. *PLOS ONE* 8: e81733, 2013.
3. **Cheung C, Marchant D, Walker EK, Luo Z, Zhang J, Yanagawa B, Rahmani M, Cox J, Overall C, Senior RM, Luo H, McManus BM.** Ablation of matrix metalloproteinase-9 increases severity of viral myocarditis in mice. *Circulation* 117: 1574–1582, 2008.
4. **Collins KA, Korcarz CE, Lang RM.** Use of echocardiography for the phenotypic assessment of genetically altered mice. *Physiol Genomics* 13: 227–239, 2003.
5. **Coronado MJ, Brandt JE, Kim E, Bucek A, Bedja D, Abston ED, Shin J, Gabrielson KL, Mitzner W, Fairweather D.** Testosterone and interleukin-1β increase cardiac remodeling during coxsackievirus B3 myocarditis via serpin A 3n. *Am J Physiol Heart Circ Physiol* 302: H1726–H1736, 2012.
6. **DeFea KA, Zalevsky J, Thoma MS, Déry O, Mullins RD, Bunnett NW.** β-Arrestin-dependent endocytosis of proteinase-activated receptor 2 is required for intracellular targeting of activated ERK1/2. *J Cell Biol* 148: 1267–1281, 2000.
7. **Doroshenko BH, Saliuta MIu Nazar PS, Kotko MD, Karpenko OI, Bezuhlova SV.** Fermental (plasmin) blood system in patients with acute viral myocarditis. *Lik Sprava*: 9–12, 2009.
8. **Florea VG, Anand IS.** Troponin T and plasma collagen peptides in heart failure. *Circ Heart Fail* 5: 394–397, 2012.
9. **Gearing AJ, Beckett P, Christodoulou M, Churchill M, Clements J, Davidson AH, Drummond AH, Galloway WA, Gilbert R, Gordon JL, Leber TM, Mangan M, Miller K, Nayee P, Owen K, Patel S, Thomas w Wells G, Wood LM, Woolley K.** Processing of tumor necrosis factor-a precursor by metalloproteinases. *Nature* 370: 555–557, 1994.
10. **Goldring MB, Birkhead J, Sandell LJ, Kimura T, Krane SM.** Interleukin 1 suppresses expression of cartilage-specific types II and IX collagens and increases types I and III collagens in human chondrocytes. *J Clin Invest* 82: 2026–2037, 1988.
11. **Gunja-Smith Z, Morales AR, Romanelli R, Woessner JF Jr.** Remodeling of human myocardial collagen in idiopathic dilated cardiomyopathy. Role of metalloproteinases and pyridinoline cross-links. *Am J Pathol* 148: 1639–1648, 1996.
12. **Heymans S, Pauschinger M, De Palma A, Kallwellis-Opara A, Rutschow S, Swinnen M, Vanhoutte D, Gao F, Torpai R, Baker AH, Padalko E, Neyts J, Schultheiss HP, Van de Werf F, Carmeliet P, Pinto YM.** Inhibition of urokinase-type plasminogen activator or matrix metalloproteinases prevents cardiac injury and dysfunction during viral myocarditis. *Circulation* 114: 565–573, 2006.
13. **Hirota M, Ohmuraya M, Baba H.** Genetic background of pancreatitis. *Postgrad Med J* 82: 775–778, 2006.
14. **Ing DJ, Zang J, Dzau VJ, Webster KA, Bishopric NH.** Modulation of cytokine-induced cardiac myocyte apoptosis by nitric oxide, Bak, and Bcl-x. *Circ Res* 84: 21–33, 1999.
15. **Kenyon NJ, Ward RW, McGrew G, Last JA.** TGF-β1 causes airway fibrosis and increased collagen I and III mRNA in mice. *Thorax* 58: 772–777, 2003.
16. **Kido H, Okumura Y, Takahashi E, Pan HY, Wang S, Yao D, Yao M, Chida J, Yano M.** Role of host cellular proteases in the pathogenesis of influenza and influenza-induced multiple organ failure. *Biochim Biophys Acta* 1824: 186–194, 2012.
17. **Kilkenny C, Browne W, Cuthill IC, Emerson M, Altman DG; National Centre for the Replacement, Refinement, and Reduction of Animals in Research.** Animal research: reporting in vivo experiments–the ARRIVE guidelines. *J Cereb Blood Flow Metab* 31: 991–993, 2011.
18. **Kindermann I, Barth C, Mahfoud F, Ukena C, Lenski M, Yilmaz A, Klingel K, Kandolf R, Sechtem U, Cooper LT, Böhm M.** Update on myocarditis. *J Am Coll Cardiol* 59: 779–792, 2012.
19. **Kinoh H, Sato H, Tsunezuka Y, Takino T, Kawashima A, Okada Y, Seiki M.** MT-MMP, the cell surface activator of proMMP-2 (pro-gelatinase A), is expressed with its substrate in mouse tissue during embryogenesis. *J* Cell Sci 109: 953–959, 1996.
20. **Koivunen E, Ristimäki A, Itkonen O, Osman S, Vuento M, Stenman UH.** Tumorassociated trypsin participates in cancer cell-mediated degradation of extracellular matrix. *Cancer Res* 51: 2107–2112, 1991.

21. **Koshy SK, Reddy HK, Shukla HH.** Collagen cross-linking: new dimension to cardiac remodeling. *Cardiovasc Res* 57: 594–598, 2003.
22. **Le TQ, Kawachi M, Yamada H, Shiota M, Okumura Y, Kido H.** Identification of trypsin I as a candidate for influenza A virus and Sendai virus envelope glycoprotein processing protease in rat brain. *Biol Chem* 387: 467–475, 2006.
23. **Li J, Schwimmbeck PL, Tschope C, Leschka S, Husmann L, Rutschow S, Reichenbach F, Noutsias M, Kobalz U, Poller W, Spillmann F, Zeichhardt H, Schultheiss HP, Pauschinger M.** Collagen degradation in a murine myocarditis model: relevance of matrix metalloproteinase in association with inflammatory induction. *Cardiovasc Res* 56: 235–247, 2002.
24. **Li YY, Feng YQ, Kadokami T, McTiernan CF, Draviam R, Watkins SC, Feldman AM.** Myocardial extracellular matrix remodeling in transgenic mice overexpressing tumor necrosis factor α can be modulated by anti-tumor necrosis factor α therapy. *Proc Natl Acad Sci USA* 97: 12746–12751, 2000.
25. **Lohman RJ, O'Brien TJ, Cocks TM.** Protease-activated receptor-2 regulates trypsin expression in the brain and protects against seizures and epileptogenesis. *Neurobiol Dis* 30: 84–93, 2008.
26. **López B, González A, Díez J.** Circulating biomarkers of collagen metabolism in cardiac diseases. *Circulation* 121: 1645–1654, 2010.
27. **Mackay AR, Corbitt RH, Hartzler JL, Thorgeirsson UP.** Basement membrane type IV collagen degradation: evidence for the involvement of a proteolytic cascade independent of metalloproteinases. *Cancer Res* 50: 5997–6001, 1990.
28. **Marchant D, McManus BM.** Matrix metalloproteinases in the pathogenesis of viral heart disease. *Trends Cardiovasc Med* 19: 21–26, 2009.
29. **Mason JW.** Myocarditis and dilated cardiomyopathy: an inflammatory link. *Cardiovasc Res* 60: 5–10, 2003.
30. **Mauviel A, Lapière JC, Halcin C, Evans CH, Uitto J.** Differential cytokine regulation of type I and type VII collagen gene expression in cultured human dermal fibroblasts. *J Biol Chem* 269: 25–28, 1994.
31. **Michel JB.** Anoikis in the cardiovascular system: known and unknown extracellular mediators. *Arterioscler Thromb Vasc Biol* 23: 2146–2154, 2003.
32. **Mir SA, Chatterjee A, Mitra A, Pathak K, Mahata SK, Sarkar S.** Inhibition of b signal transducer and activator of transcription 3 (STAT3) attenuates interleukin-6 (IL-6)-induced collagen synthesis and resultant hypertrophy in rat heart. *J Biol Chem* 287: 2666–2677, 2012.
33. **Moilanen M, Sorsa T, Stenman M, Nyberg P, Lindy O, Vesterinen J, Paju A, Konttinen YT, Stenman UH, Salo T.** Tumorassociated trypsinogen-2 (trypsinogen-2) activates procollagenases (MMP-1, -8, -13) and stromelysin-1 (MMP-3) and degrades type I collagen. *Biochemistry* 42: 5414–5420, 2003.
34. **Nhu QM, Shirey K, Teijaro JR, at al Antalis TM, Fasano A, Vogel SN.** Novel signaling interactions between proteinase-activated receptor 2 and Toll-like receptors in vitro and in vivo. *Mucosal Immunol* 3: 29–39, 2010.
35. **Niu QX, Chen HQ, Chen ZY, Fu YL, Lin JL, He SH.** Induction of inflammatory cytokine release from human umbilical vein endothelial cells by agonists of proteinase-activated receptor-2. *Clin Exp Pharmacol Physiol* 35: 89–96, 2008.
36. **Okada Y, Gonoji Y, Naka K, Tomita K, Nakanishi I, Iwata K, Yamashita K, Hayakawa T.** Matrix metalloproteinase 9 (92-kDa gelatinase/type IV collagenase) from HT 1080 human fibrosarcoma cells. Purification and activation of the precursor and enzymic properties. *J Biol Chem* 267: 21712–21719, 1992.
37. **Okada Y, Naka K, Kawamura K, Matsumoto T, Nakanishi I, Fujimoto N, Sato H, Seiki M.** Localization of matrix metalloproteinase 9 (92-kilodalton gelatinase/type IV collagenase = gelatinase B) in osteoclasts: implications for bone resorption. *Lab Invest* 72: 311–322, 1995.
38. **Onyimba JA, Coronado MJ, Garton AE, Kim JB, Bucek A, Bedja D, Gabrielson KL, Guilarte TR, Fairweather D.** The innate immune response to coxsackievirus B3 predicts progression to cardiovascular disease and heart failure in male mice. *Biol Sex Differ* 2: 2, 2011.
39. **Pan HY, Yamada H, Chida J, Wang S, Yano M, Yao M, Zhu J, Kido H.** Up-regulation of ectopic trypsins in the myocardium by influenza A virus infection triggers acute myocarditis. *Cardiovasc Res* 89: 595–603, 2011.
40. **Pan HY, Yano M, Kido H.** Effects of inhibitors of Toll-like receptors, protease-activated receptor-2 signalings and trypsin on influenza A virus replication and up-regulation of cellular factors in cardiomyocytes. *J Med Invest* 58: 19–28, 2011.
41. **Pauschinger M, Knopf D, Petschauer S, Doerner A, Poller W, Schwimmbeck PL, Kühl U, Schultheiss HP.** Dilated cardiomyopathy is associated with significant changes in collagen type I/III ratio. *Circulation* 99: 2750–2756, 1999.
42. **Prabhu SD.** Cytokine-induced modulation of cardiac function. *Circ Res* 95: 1140–1153, 2004.
43. **Rapala KT, Vähä-Kreula MO, Heino JJ, Vuorio EI, Laato MK.** Tumor necrosis factor-α inhibits collagen synthesis in human and rat granulation tissue fibroblasts. *Experientia* 52: 70–74, 1996.
44. **Rosa'rio HS, Waldo SW, Becker S, Schmid-Schönbein GW.** Pancreatic trypsin increases matrix metalloproteinase-9 accumulation and activation during acute intestinal ischemia-reperfusion in the rat. *Am J Pathol* 164: 1707–1716, 2004.
45. **Satoh M, Nakamura M, Akatsu T, Shimoda Y, Segawa I, Hiramori K.** Myocardial osteopontin expression is associated with collagen fibrillogenesis in human dilated cardiomyopathy. *Eur J Heart Fail* 7: 755–762, 2005.
46. **Schnitt SJ, Stillman IE, Owings DV, Kishimoto C, Dvorak HF, Abelmann WH.** Myocardial fibrin deposition in experimental viral myocarditis that progresses to dilated cardiomyopathy. *Circ Res* 72: 914–920, 1993.
47. **Sharma A, Tao X, Gopal A, Ligon B, Andrade-Gordon P, Steer ML, Perides G.** Protection against acute pancreatitis by activation of protease-activated receptor-2. *Am J Physiol Gastrointest Liver Physiol* 288: G388–G395, 2005.
48. **Tatsumi T, Akashi K, Keira N, Matoba S, Mano A, Shiraishi J, Yamanaka S, Kobara M, Hibino N, Hosokawa S, Asayama J, Fushiki S, Fliss H, Nakagawa M, Matsubara H.** Cytokine-induced nitric oxide inhibits mitochondrial energy production and induces myocardial dysfunction in endotoxin-treated rat hearts. *J Mol Cell Cardiol* 37: 775–784, 2004.
49. **Ukimura A, Satomi H, Ooi Y, Kanzaki Y.** Myocarditis associated with influenza A H1N1pdm2009. *Influenza Res Treat* 2012: 351979, 2012.
50. **Wang S, Le TQ, Kurihara N, Chida J, Cisse Y, Yano M, Kido H.** Influenza virus-cytokine-protease cycle in the pathogenesis of vascular hyperpermeability in severe influenza. *J Infect Dis* 202: 991–1001, 2010.
51. **Wang S, Quang Le T, Chida J, Cisse Y, Yano M, Kido H.** Mechanisms of matrix metalloproteinase-9 up-regulation and tissue destruction in various organs in influenza A virus infection. *J Med Invest* 57: 26–34, 2010.
52. **Weithauser A, Bobbert P, Antoniak S, Böhm A, Rauch BH, Klingel K, Savvatis K, Kroemer HK, Tschope C, Stroux A, Zeichhardt H, Poller W, Mackman N, Schultheiss HP, Rauch U.** Protease-activated receptor-2 regulates the innate immune response to viral infection in a coxsackievirus B3-induced myocarditis. *J Am Coll Cardiol* 62: 1737–1745, 2013.
53. **Westermann D, Savvatis K, Schultheiss HP, Tschöpe C.** Immunomodulation and matrix metalloproteinases in viral myocarditis. *J Mol Cell Cardiol* 48: 468–473, 2010.
54. **Yamamoto K, Masuyama T, Sakata Y, Nishikawa N, Mano T, Yoshida J, Miwa T, Sugawara M, Yamaguchi Y, Ookawara T, Suzuki K, Hori M.** Myocardial stiffness is determined by ventricular fibrosis, but not by compensatory or excessive hypertrophy in hypertensive heart. *Cardiovasc Res* 55: 76–82, 2002.

Avens Publishing Group
J Vaccine Immunotechnology
January 2015 Volume 2, Issue 1

Open Access Research Article

Journal of Vaccine & Immunotechnology

Oral Administration of *Lactobacillus pentosus* Strain S-PT84 Enhances Anti-Influenza Virus-Specific IgG Production in Plasma after Limited Dose of Influenza Virus Vaccination in Mice

Toshihiro Maekawa[1]*, Takashi Kimoto[2], Dai Mizuno[3], Yuichi Furukawa[1], Masayuki Ida[1], Etsuhisa Takahashi[4], Takayuki Izumo[1], Yoshiko Ono[1], Hiroshi Shibata[1] and Hiroshi Kido[4]

[1]*Institute for Health Care Science, Suntory Wellness Limited, Mishima-gun, Osaka, Japan*
[2]*Department of Hygienic Sciences, Kobe Pharmaceutical University, Hyogo, Japan*
[3]*Department of Bio Analytical Chemistry, Research Institute of Pharmaceutical Sciences, Musashino University, Nishitokyo-shi, Tokyo, Japan*
[4]*Division of Enzyme Chemistry, Institute for Enzyme Research, The University of Tokushima, Tokushima, Japan*

Address for Correspondence
Toshihiro Maekawa, Institute for Health Care Science, Suntory Wellness Limited, 1-1-1 Wakayama-dai, Shimamoto-cho, Mishima-gun, Osaka 618-8503, Japan, Tel: +81-75-962-6207; Fax: +81-75-962-1690; E-mail: Toshihiro_Maekawa@suntory.co.jp

Submission: 27 November 2014
Accepted: 23 December 2014
Published: 29 December 2014

Reviewed & Approved by: Dr. Sherven Sharma, Professor of Medicine, David Geffen School of Medicine, University of California, USA

Keywords: Influenza vaccine; *Lactobacillus pentosus* strain S-PT84; Adjuvant effect; IgG; IgA

Abstract

Background: It has been reported that various *Lactobacillus* species enhance antigen-specific antibody production after viral infection and/or vaccination in animals and humans. In this study, the effect of oral administration of *Lactobacillus pentosus* strain S-PT84 on subcutaneous administration of limited dose of 2.5 ng of influenza A virus (IAV) (H1N1) split hemagglutinin (HA) vaccine was studied in mice.

Methods: Seven-week-old BALB/c female mice were fed the AIN-93M diet with or without 0.186% S-PT84 for 6 weeks ad libitum and then given subcutaneous injection of IAV/California/7/2009 (H1N1) HA vaccine at doses of 2.5–15.0 ng/mice and boosted on day 28. Two weeks after the last vaccination, the mice were sacrificed under anesthesia, and the amount of anti-HA-specific IgG in plasma was measured by ELISA.

Results: The levels of anti-HA-specific IgG in plasma were significantly higher in the S-PT84 group than in the control group without S-PT84 treatment. Anti-HA-specific IgA levels in nasal washes were under the detection level in both groups.

Conclusion: Oral administration of S-PT84 enhanced the production of HA-specific IgG antibody in plasma after subcutaneous vaccination, even at the limited dose of 2.5 ng of IAV (H1N1) HA in mice, suggesting that S-PT84 has a potent adjuvant activity against IAV HA.

Introduction

Influenza is an acute viral infection that results in high morbidity and significant mortality, particularly in infants and the elderly populations [1]. They sometimes have a high risk of fatal influenza pneumonia and thus vaccination is recommended for prevention. The World Health Organization has recommended use of oseltamivir (Tamiflu®, Chugai Pharmaceutical Co., Ltd, Tokyo, Japan) and zanamivir (Relenza®, Glaxo Smith Kline K.K., Tokyo, Japan) for the treatment of influenza. These antiviral neuraminidase inhibitors are useful options for seasonal influenza infections in the world [2]. However, Shinahara et al. recently reported that administration of these inhibitors decreases anti-IAV HA-specific IgG and IgA production in plasma and nasopharyngeal secretions, probably because of inhibition of viral replication and limited production of viral antigens [3]. The limited viral antigens do not induce sufficient acquired immunity in patients treated with anti-viral neuraminidase inhibitors, resulting in a high frequency of influenza virus re-infection in the subsequent year [3].

Lactic acid bacteria (LAB) are widely used as a health food ingredient and could modulate mucosal and systemic immune responses [4,5]. Oral administration of live *Lactobacillus casei* Shirota significantly increases the survival rate of neonatal and infant mice infected with IAV by stimulating IL-12 production and NK activity in the lung [6]. Oral administration of heat-killed *Lactobacillus plantrum* L-137 [7] and *Lactobacillus pentosus* strain b240 [8] enhances type 1 interferon production and increases the production of anti-IAV IgG in plasma and IgA in bronchoalveolar lavage fluid, respectively, and prolongs the survival period of mice infected with IAV. These studies showed that oral administration of live and nonviable *Lactobacillus* species enhances the protective effects against airway infection of IAV.

It has recently been reported that oral administration of probiotic LAB enhances vaccination-induced antibody production. *Lactobacillus acidophilus* enhances rotavirus-specific antibody after vaccination of rotavirus in the neonatal gnotobiote pig [9]. Davidson et al. reported that volunteers receiving *Lactobacillus* GG show higher protective titers after administration of live attenuated IAV/H3N2 vaccine compared to a placebo group after vaccination [10]. Moreover, Boge et al. reported that daily consumption of a probiotic drink increases relevant specific antibody responses to influenza

Citation: Maekawa T, Kimoto T, Mizuno D, Furukawa Y, Ida M, et al. Oral Administration of *Lactobacillus pentosus* Strain S-PT84 Enhances Anti-Influenza Virus-Specific IgG Production in Plasma after Limited Dose of Influenza Virus Vaccination in Mice. J Vaccine Immunotechnology. 2015;2(1): 5.

vaccination in healthy volunteers over 70 years of age [11]. Therefore oral administration of *Lactobacillus* species might be effective in preventing influenza virus infection by stimulating antibody production.

We previously reported that *Lactobacillus pentosus* strain S-PT84 enhances splenic natural killer (NK) activity and exhibits anti-allergic effects by modulating T-helper1/T-helper2 (Th1/Th2) balance [12]. Moreover, it has been reported that oral administration of S-PT84 enhances interferon-α production from plasmacytoid dendritic cells against an insufficient dose of hemagglutinating virus of Japan (HVJ) infection [13], and that intranasal administration of S-PT84 protects against influenza infection [14]. However, the effects of S-PT84 ingestion on limited dose of IAV HA vaccination and HA-specific antibody induction have not yet been examined. In this study, the effect of oral administration of S-PT84 on the induction of IAV HA-specific antibody in mice immunized by IAV HA vaccine in the nanogram range was investigated.

Materials and Methods

Animals

BALB/c female mice, 7 weeks old, were obtained from Japan SLC, Inc. (Shizuoka, Japan). Mice were housed and fed a commercial diet (CE-2) and tap water ad libitum for 1 week at 25±1 °C and 60% ± 5% humidity under a 12 h light-dark cycle before experimentation. Experiments were performed according to the Guide for the Care and Use of Laboratory Animals (NIH Publication No. 85-23, 1996).

Bacterial strains and bacteria preparation

S-PT84 was isolated from Kyoto pickles "SHIBAZUKE" [12] and was cultivated in a medium containing glucose and yeast extract (Aromild™, SK yeast extract Hi-K) at 37 °C for 24 hours. Cultured bacteria were collected by centrifugation at 9,190 x g for 5 min, washed twice with sterile saline and once with distilled water, and heat-killed at 95 °C for 5 min. Heat-killed S-PT84 was lyophilized for use in the experiments.

Vaccine

The influenza antigen used in the present studies, IAV/California/7/2009(H1N1) virus processed for HA vaccine (split-product, 0.636 μg protein/0.341 μg HA/mL), was purchased from DENKA SEIKEN Co., Ltd. (Tokyo, Japan).

Procedure and sample collection

BALB/c mice were fed on a commercial diet (AIN-93M, Oriental Yeast Co. Ltd., Tokyo, Japan) with or without 0.186% S-PT84 and tap water ad libitum for 6 weeks. Mice were given subcutaneous vaccinations (2.5–15.0 ng HA/100 μL) and boosted on day 28. Two weeks after the last vaccination, the mice were sacrificed under anesthesia. Blood samples were collected from the vein. Blood was centrifuged (2,500 *g*, 10 min) at 4 °C, and the supernatant was collected.

Enzyme-linked immunosorbent assay (ELISA)

Anti-influenza HA-specific antibodies in plasma were measured by ELISA [15]. Briefly, 96-well plates (Nunc, Naperville, IL) were coated with HA vaccine and bovine serum albumin (BSA, 0.1 μg/well each) in PBS overnight at 4 °C. After the pre-coating, it was blocked with 1% BSA in 50 mM Tris-HCl (pH 8.0) containing 0.14 M NaCl and 0.05% Tween 20 (TTS) for 1 hour at room temperature. The plasma diluted with TTS containing 1% BSA was added to each well and incubated for 3 hours at room temperature. The plate was washed six times with TTS containing 1% BSA and incubated with goat anti-mouse IgG antibodies conjugated with horseradish peroxidase (Bethyl Laboratories Inc., Montgomery, TX, USA) for 2 hours at room temperature. Color was developed by the addition of TMB substrate (Bethyl Laboratories), according to the instructions provided by the manufacturer. The chromogen produced was measured at 450 nm using a SPECTRA max PLUS384 AutoReader (Molecular Devices, Tokyo, Japan). Antibody titers were defined as the reciprocal of the highest dilution of sample for which the optical density (OD) was at least twice the OD of the negative control samples before vaccination.

Statistical analysis

The significance of differences in values between the control group and S-PT84 group was determined using Student's t-test. P-values less than 0.05 were considered significant.

Results

Doses of vaccination of IAV/California/7/2009(H1N1)

The induced levels of HA-specific IgG antibody in plasma were analyzed to detect the optimal dose of IAV/California/7/2009(H1N1) to evaluate the effect of *Lactobacillus pentosus* S-PT84 as an adjuvant. HA-specific IgG antibody in plasma was increased by IAV HA vaccination in a dose-dependent manner in the range between 2.5 and 15.0 ng (Figure 1). HA at 2.5 ng, even at the lowest dosage, could induce production of HA-specific IgG in plasma, and that dose may be appropriate for examining the effect of LAB on enhancing HA-specific IgG production in plasma. Therefore, the minimal dose of 2.5 ng HA was used to investigate the adjuvant effect of LAB.

Effect of *Lactobacillus pentosus* S-PT84 on the production of HA-specific IgG in plasma

Mice were fed the AIN-93M diet with or without 0.186% S-PT84 for 6 weeks. In the control group treated with two subcutaneous injections of IAV HA at 2.5 ng alone, a small amount of antigen-specific IgG antibody production was detected in plasma. The S-PT84 group of mice treated with continuous feeding of the AIN-93M diet with 0.186% S-PT84 during the experimental period also received two subcutaneous injections of IAV HA at 2.5 ng. HA-specific IgG antibody levels in plasma were higher in the S-PT84 group than in the control group (Figure 2A). On the other hand, HA-specific IgA in nasal washes was under detection levels in both groups (data not shown). The induced HA-specific IgG titers in plasma were significantly higher in the S-PT84 group than in the control group (p=0.007) (Figure 2B).

Discussion

In this study, oral administration of S-PT84 enhanced HA-specific IgG induction in plasma, but not HA-specific IgA induction in nasal wash, after subcutaneous administration of limited dose of IAV (H1N1) HA in mice. The findings suggest that S-PT84 has an adjuvant effect against IAV HA on plasma IgG induction, even at minimal dose. Nonaka et al. reported that S-PT84 induces cytokine

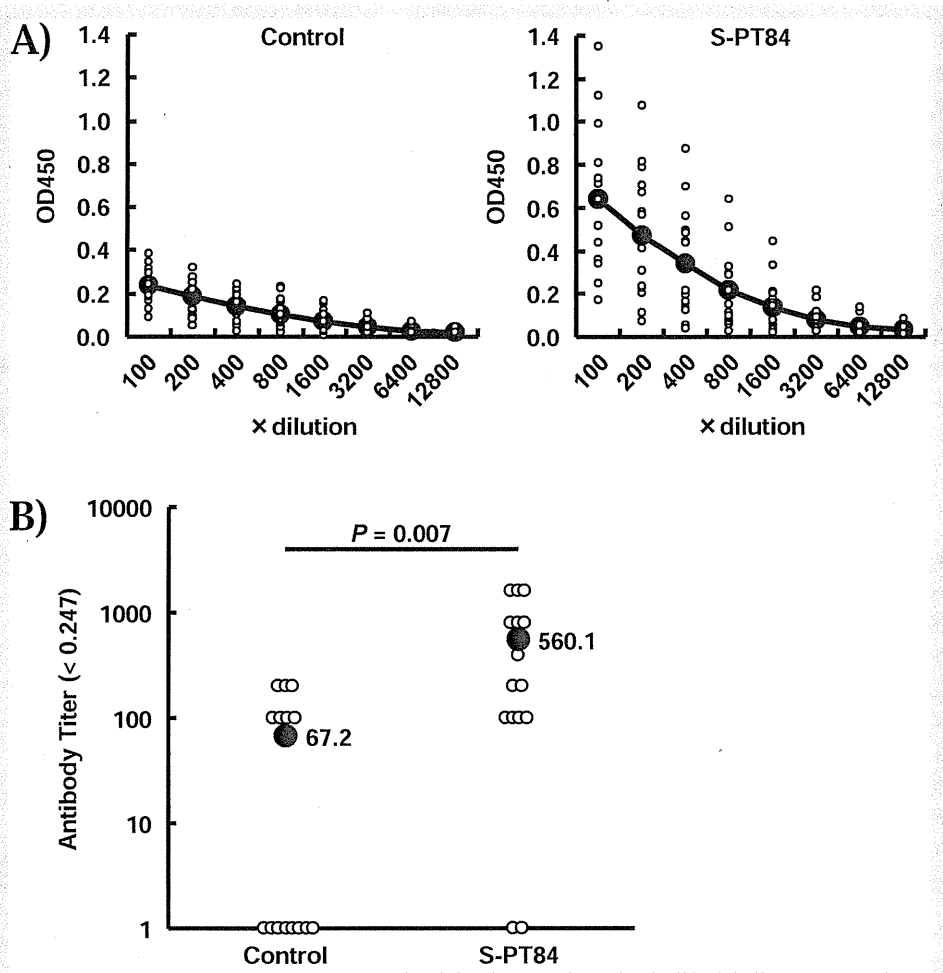

Figure 2: Effect of *Lactobacillus pentosus* strain S-PT84 on HA-specific IgG production by vaccination. Mice were fed an AIN-93M diet with or without 0.186% S-PT84 for 6 weeks followed by subcutaneous vaccination of 2.5 ng HA and boosted on day 28 from the initial vaccination. Two weeks after the last vaccination, plasma was collected from each mouse, and the amount of HA-specific IgG Antibody (Ab) **(A)** was measured by ELISA and expressed as the titer **(B)**, as described in Materials and Methods. Values are means of 15 mice in each group. Significant differences are seen between the control group and the S-PT84 group. Open circles are individual data, closed circles are mean values.

Japan is becoming a super-aging society more rapidly than other countries. Elderly persons have a high risk of influenza-associated pneumonia, which is sometimes fatal. Thus, management of influenza outbreaks is important for them. Indeed, seroconversion and seroprotection are lower in elderly individuals than in adults after influenza vaccination, and their immune functions are weaker than in adults [20]. It is important that preventive action be taken to enhance immune function or provide vaccination for the elderly. In this regard, S-PT84 may have a potential to improve their immune response.

References

1. Gillim-Ross L, Subbarao K (2006) Emerging respiratory viruses: challenges and vaccine strategies. Clin Microbiol Rev 19: 614-636.
2. Moscona A (2005) Neuraminidase inhibitors for Influenza. N Engl J Med 353: 1363-1373.
3. Shinahara W, Takahashi E, Sawabuchi T, Arai M, Hirotsu N, et al. (2013) Immunomodulator clarithromycin enhances mucosal and systemic immune responses and reduces re-infection rate in pediatric patients with Influenza treated with antiviral neuraminidase inhibitors: A retrospective analysis. PLoS One 8: e70060.
4. Blum S, Haller D, Pfeifer A, Schiffrin EJ (2002) Probiotics and immune response. Clin Rev Allergy Immunol 22: 287-309.
5. Perdigón G, Fuller R, Raya R (2001) Lactic acid bacteria and their effect on the immune system. Curr Issues Intest Microbiol 2: 27-42.
6. Yasui H, Kiyoshima J, Hori T (2004) Reduction of influenza virus titer and protection against influenza virus infection in infant mice fed *Lactobacillus casei* Shirota. Clin Diagn Lab Immunol 11: 675-679.
7. Maeda N, Nakamura R, Hirose Y, Murosaki S, Yamamoto Y, et al. (2009) Oral administration of heat-killed *Lactobacillus plantarum* L-137 enhances protection against influenza virus infection by stimulation of type I interferon production in mice. Int Immunopharmacol 9: 1122-1125.
8. Kobayashi N, Saito T, Uematsu T, Kishi K, Toba M, et al. (2011) Oral administration of heat-killed *Lactobacillus pentosus* strain b240 augments protection against influenza virus infection in mice. Int Immunopharmacol 11: 199-203.
9. Zhanga W, Azevedoa MSP, Wenb K, Gonzaleza A, Saifa LJ, et al. (2008) Probiotic *Lactobacillus acidophilus* enhances the immunogenicity of an oral rotavirus vaccine in gnotobiotic pigs. Vaccine 26: 3655-3661.

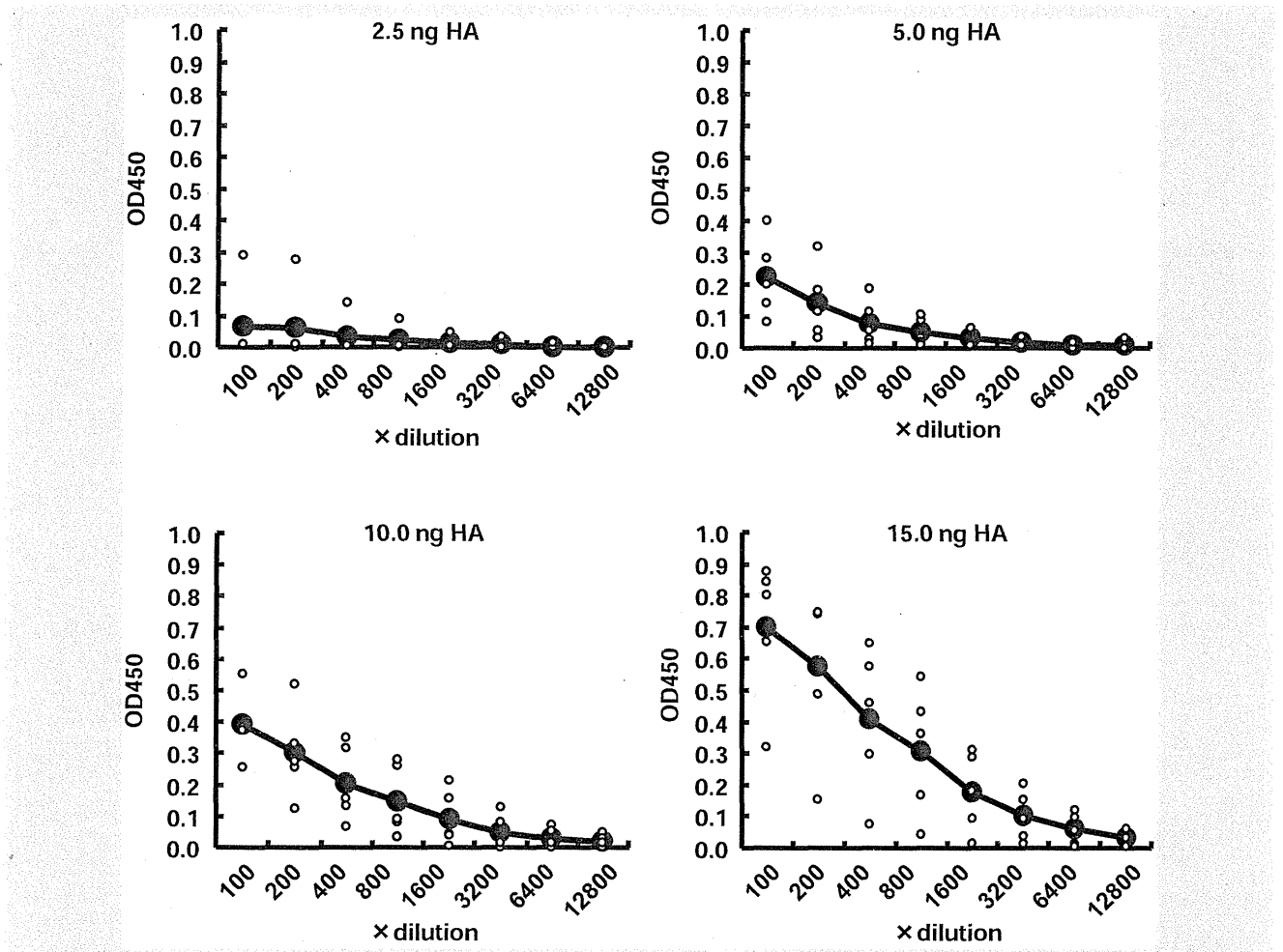

Figure 1: The amount of HA-specific IgG production by vaccination. Mice were fed an AIN-93M diet and given subcutaneous vaccination at doses between 2.5 and 15.0 ng HA and boosted on day 28 from the initial vaccination. Two weeks after the last vaccination, plasma was collected from each mouse, and the amount of HA-specific IgG antibody was measured by ELISA, as described in Materials and Methods. Values are means of 5 mice in each group. Open circles are individual data, closed circles are mean values.

production from peritoneal macrophages in vitro and enhances the activity of NK cells *in vivo* [12]. Koizumi et al. also reported that S-PT84 stimulates IFN-γ and IL-12 production through Toll-like receptor (TLR)-2 and TLR-4 on dendritic cells [16]. Moreover, Izumo et al. reported that *Salmonella*-specific antibody is enhanced by S-PT84 ingestion in *Salmonella* typhimurium-infected mice [17]. Accordingly, we thought that antigen-presenting cells were activated by ingestion of S-PT84 in this experiment, and production of HA-specific IgG in plasma may be enhanced, as in a previous report [17]. It is well known that influenza vaccines administered intramuscularly or subcutaneously induce a predominantly IgG-mediated protection in the systemic immune compartment, but this systemic immunization offers inadequate induction of IgA in airway mucosa [18]. Therefore, oral administration of S-PT84 might affect HA antigen-induced dendritic cell-mediated systemic immunity and induce HA-specific IgG in plasma, but not affect mucosal immunity and HA-specific IgA production.

The present data suggest that S-PT84 enhances antibody production as an adjuvant with limited dose of influenza viral antigen. Hui-Tsu et al. reported that the induction of HA-specific antibody in plasma was enhanced by IAV HA (H1N1) vaccination at 10 ng dose in mice, and the survival rate was also significantly improved by this vaccination [19]. The optimal density (OD) level of HA-specific IgG was similar compared with our present study. Moreover, the strain of IAV/California/7/2009 (H1N1) was same in both experiments. Therefore, we speculate that HA-specific antibody production level by the killed bacterial adjuvant S-PT84 might be sufficient for the viral protection and then an ample titer was obtained for influenza virus exclusion. It suggests that S-PT84 may decrease the risk of influenza virus re-infection treated with anti-viral neuraminidase inhibitors.

As a next step, it should be to investigate whether oral administration of S-PT84 together with the vaccination on limited dose of HA antigen can protect IAV infection, and/or whether oral administration of S-PT84 can induce sufficiently HA-specific IgG antibody treated with antiviral neuraminidase inhibitors after IAV infection.

10. Davidson LE, Fiorino A-M, Snydman DR, Hibberd PL (2011) Lactobacillus GG as an immune adjuvant for live attenuated influenza vaccine in healthy adults: a randomized double blind placebo controlled trial. Eur J Clin Nutr 65: 501-507.

11. Boge T, Rémigy M, Vaudaine S, Tanguyc J, Bourdet-Sicardc R, et al. (2009) A probiotic fermented dairy drink improves antibody response to influenza vaccination in the elderly in two randomised controlled trials. Vaccine 27: 5677-5684.

12. Yuji N, Takayuki I, Fumi I, Toshihiro M, Hiroshi S, et al. (2008) Antiallergic effects of *Lactobacillus pentosus* strain S-PT84 mediated by modulation of Th1/Th2 immunobalance and induction of IL-10 production. Int Arch Allergy Immunol 145: 249-257.

13. Izumo T, Maekawa T, Ida M, Kishi A, Akatani K, et al. (2011) Effect of *Lactobacillus pentosus* S-PT84 ingestion on IFN-α production from plasmacytoid dendritic cells by virus stimulation. Biosci Biotechnol Biochem 75: 370-372.

14. Izumo T, Maekawa T, Ida M, Noguchi A, Kitagawa Y, et al. (2010) Effect of intranasal administration of *Lactobacillus pentosus* S-PT84 on influenza virus infection in mice. Int Immunopharmacol 10: 1101-1106.

15. Nishino M, Mizuno D, Kimoto T, Shinahara W, Fukuta A, et al. (2009) Influenza vaccine with surfacten, a modified pulmonary surfactant, induces systemic and mucosal immune responses without side effects in minipigs. Vaccine 27: 5620-5627.

16. Koizumi S, Wakita D, Sato T, Mitamura R, Izumo T, et al. (2008) Essential role of Toll-like receptors for dendritic cell and NK1.1(+) cell-dependent activation of type 1 immunity by *Lactobacillus pentosus* strain S-PT84. Immunol Lett 120: 14-19.

17. Izumo T, Izumi f, Nakagawa I, Kitagawa Y, Sibata H, et al. (2011) Influence of *Lactobacillus pentosus* S-PT84 ingestion on the mucosal immunity of healthy and *Salmonella* typhimurium-infected mice. Biosci Microflora 30: 27-35.

18. Kimoto T, Mizuno D, Takei T, Kunimi T, Ono S, et al. (2013) Intranasal influenza vaccination using a new synthetic mucosal adjuvant SF-10: induction of potent local and systemic immunity with balanced Th1 and Th2 responses. Influenza Other Respir Viruses 7: 1218-1226.

19. Lin HT, Chuang CC, Wu HL, Chu DM, Wang YC (2013) Characterization of cross protection of Swine-Origin Influenza Virus (S-OIV) H1N1 and reassortant H5N1 influenza vaccine in BALB/c mice given a single-dose vaccination. J Biomed Sci 20: 19.

20. Goodwin K, Viboud C, Simonsen L (2006) Antibody response to influenza vaccination in the elderly: A quantitative review. Vaccine 24: 1159-1169.

Acta Med. Nagasaki 58: 103－111

SAM domain-containing N-terminal region of SAMHD1 plays a crucial role in its stabilization and restriction of HIV-1 infection

Sayuri SHIGEMATSU, Hideki HAYASHI, Kiyoshi YASUI, Toshifumi MATSUYAMA

Division of Cytokine Signaling, Department of Molecular Microbiology and Immunology, Graduate School of Biomedical Sciences, Nagasaki University, Nagasaki, Japan

SAMHD1 restricts human immunodeficiency virus type 1 (HIV-1) infection in a cell-type specific manner. Other than primary monocyte derived cells and resting $CD4^+$ T cells, the SAMHD1-mediated HIV-1 block was reported only in phorbol 12-myristate 13-acetate (PMA)-differentiated THP-1 and U937 monocyte cell lines. We previously reported that SAMHD1 restricted HIV-1 infection in TE671 rhabdomyosarcoma cells in addition to these cell lines. In this study, we compared the amounts of the full-length SAMHD1 and its deletion mutants, SAM domain containing N-terminal fragment (residues 1-119, SAMHD1n) and HD domain containing C-terminal fragment (120-626, SAMHD1c) in U937, TE671, and HeLa cells. The results showed that the full-length SAMHD1 and SAMHD1n proteins were significantly more abundant than the SAMHD1c protein in TE671 and differentiated U937 cells. The proteasome inhibitor MG132 increased the amount of the SAMHD1c and the SAMHD1c-fused GFP proteins. In contrast, the fusion of the SAMHD1n to the APOBEC3G protein inhibited Vif-induced proteasomal degradation in TE671 and in differentiated U937 cells. These results indicated that the SAMHD1 C-terminal HD domain-containing region leads the SAMHD1 to proteasomal degradation, and the SAMHD1 N-terminal SAM domain-containing region stabilizes the protein. Our study showed that the SAMHD1 protein expression is post-translationally regulated and the significance of SAM and HD domains for the full-length SAMHD1 protein stability. Further, we suggest that the SAM domain-containing N-terminal region participate in the cell-type specific restrictive function of SAMHD1 against HIV-1 infection, by protein stabilization.

ACTA MEDICA NAGASAKIENSIA 58: 103－111, 2014

Key words: SAMHD1; HIV; restriction factor; interferon-inducible gene; proteasome degradation; ubiquitination

Introduction

SAMHD1 (1-626 aa), composed of a tandemly linked-SAM domain (45-110 aa) and HD domain (164-319 aa), has recently been identified as a restriction factor against HIV-1. SAMHD1 was originally identified as a human homolog of mouse *Mg11* isolated from IFNγ-stimulated mouse dendritic cells [1,2], suggesting that SAMHD1 is an IFN-stimulated gene [3,4] though it depends on cell-type [3,5].

In parallel to the hosts obtaining restriction factors, viruses have developed mechanisms to overcome these restriction factors. Vpx, encoded by HIV-2 and simian immunodeficiency viruses (SIVs) but not by HIV-1 [6,7,8,9,10], is a potent counterpart of SAMHD1. These Vpx proteins bind to the SAMHD1 C-terminal motif (606-626 aa) and deliver the complex to the $CRL4^{DCAF1}$ ubiquitin E3 ligase [11] for subsequent proteasome-dependent degradation.

HD domain contains a catalytic core for hydrolysis activity and the several reports showed that the HD domain-containing C-terminal region of SAMHD1 (120-626 aa) inhibits HIV-1 reverse transcription (RT) by its dGTP dependent deoxynucleoside triphosphate-triphosphatase (dGTP triphosphatase)

Address correspondence: Division of Cytokine Signaling, Department of Molecular Microbiology and Immunology, Nagasaki University Graduate School of Biomedical Science, 1-12-4 Sakamoto, Nagasaki 852-8523, Japan
Phone: +81-95-819-7081, FAX: +81-95-819-7083, E-mail: tosim@net.nagasaki-u.ac.jp

Received September 2, 2013; Accepted December 26, 2013

activity [12,13]. In addition, recombinant SAMHD1 protein possesses 3' to 5' exonuclease activities against DNAs and RNAs, as well as nucleic acids and viral genome binding abilities in which the SAM domain containing N-terminal region (1-118 aa) plays a crucial role [14].

Interestingly, various cell lines endogenously express the SAMHD1 [1,6,7], but SAMHD1 can inhibit HIV-1 infection only in terminally differentiated myeloid cells, such as PMA-differentiated THP-1 [6,9,15], monocyte-derived macrophages (MDMs) [13] and monocyte-derived dendritic cells (MDDCs) [6,7,13], and resting $CD4^+$ T cells [8,16] but not in undifferentiated THP-1 and HEK293T cells [7]. Exogenously over-expressed SAMHD1 restricted the infection in PMA-differentiated U937 macrophage cells but not in undifferentiated U937 and HeLa cells [3]. Thus, there are unknown mechanism(s) contributing to the cell type-specific HIV-1 restriction by SAMHD1.

Meanwhile, the protection of innate immunity-associated proteins from ubiquitination and degradation, *i.e.*, protein stabilization, is one of the mechanisms to induce innate immune signaling. For example, Lee *et al.* [17] recently showed that the TBK1 protein, a key mediator in type I IFN expression, is stabilized by CDC37 in IFN-stimulated DNA and retrovirus sensing. Korczeniewska *et al.* [18] showed that the COP9 signalosome stabilizes the IFN regulatory factor 5 (IRF5) protein, an important role player in the induction of type I IFNs and proinflammatory cytokines. Thus, protein stabilization is a critical event in innate immunity.

To understand the involvement of SAMHD1 stabilization in the SAMHD1-induced cell-type specific HIV-1 infection restriction, we analyzed the expression levels and stability of the full-length SAMHD1 protein and its deletion mutants in U937, TE671, and HeLa cells. We describe supporting evidences for SAMHD1 is post-translationally regulated and the significance of SAM domain-containing and HD domain-containing region for the SAMHD1 protein stability.

Materials and Methods

Cells. THP-1 and U937 cells were grown in RPMI medium (Wako) at 37 °C in a 5% CO_2 incubator. HeLa and TE671 cells were grown in Dulbecco's modified Eagle medium (D-MEM) (Wako). Both media were supplemented with 8% heat-inactivated fetal bovine serum (FBS) (PAA Laboratories GmbH) and 1 % penicillin-streptomycin (Sigma-Aldrich). Unless indicated, all cells were seeded at $1x10^6$ cells per 6 cm culture-dish. At 24 hrs after transfection, U937 cells were stimulated by phorbol 12-myristate 13-acetate (PMA) at various concentrations, to promote differentiation into macrophages.

Real-time PCR

THP-1 cells were seeded in 24-well dishes (1x105/well), and total RNA samples were prepared by Trizol Reagent (Ambicon) after differentiation with 30, 50, and 500 ng/ml PMA for 48 hrs. Semi-quantitative RT-PCR was performed with a high fidelity RT-PCR kit (TAKARA). Real-time PCR was performed with M-MLV reverse transcriptase (NEB). A SYBR Green PCR kit (TOYOBO) was used to quantitate the PCR products on the ABI PRISM 7900HT real-time PCR detection system. The amounts of the SAMHD1 PCR products were normalized by those of the GAPDH PCR products. The nucleotide sequences of the primers for the SAMHD1 mRNA were 5'-AGCGATTGGTTCAAATCCAC-3' and 5'-TCGATTGTGTGAAGCTCCTG-3', and for the GAPDH mRNA were 5'-GAGTCAACGGATTTGGTCGT-3' and 5'-TTGATTTTGGAGGGATCTCG-3'.

Plasmids. The C-terminally HA epitope-tagged full-length SAMHD1 (1-626 aa), SAMHD1n (1-119 aa), and SAMHD1c (120-626 aa) expression plasmids were constructed by amplifying each sequence from the full-length SAMHD1 expression plasmid (OriGene Technologies), as a template. The pcDNA3.1 vector was purchased from Invitrogen.

The PCR primers for amplifying the full-length HA-tagged SAMHD1 sequence were a forward primer 5'-GTGTAGCCATGCAGCGA-3' (SAMHD1 F) and a reverse primer, 5'-TCATGCGTAATCCGGAACATCGTACGGGTACATTGGGTCATCTTTAAAAAGCTG-3' (SAMHD1-HA-R); for HA-tagged SAMHD1n sequence, the SAMHD1 F primer and a reverse primer, 5'-TCATGCGTAATCCGGAACATCGTACGGGTAATTAATTACCTTCATTGTATC-3'; and for HA-tagged SAMHD1c sequence, a forward primer, 5'-GTAGCCATGGATCCTATCCATGGCCAC-3', and the SAMHD1-HA-R primer. Each PCR product was inserted into the pcDNA3.3-TOPO vector (Invitrogen).

An enhanced green fluorescent protein (EGFP) expression plasmid was generated in our laboratory. The EGFP stop codon was replaced by an *Eco*RI sequence in the EGFP expression plasmid (EGFP-EcoRI). To construct the C-terminally SAMHD1c-fused EGFP expression plasmid (GFP-HD), the HD region was amplified by PCR, using the SAMHD1c-HA expression plasmid as the template, with the *Eco*RI sequence-containing forward primer, 5'-TTATTAGAATTCGATCCTATCCATCATCAC-3', and the *Xho*I

sequence-containing reverse primer, 5'-TTATTACTCGAGTCACATTGGGTCATCTTT-3'. The PCR product was digested with the *Eco*RI and *Xho*I restriction enzymes and inserted into the EGFP-EcoRI plasmid at the *Eco*RI and *Xho*I sites.

The expression plasmid for C-terminally Myc-tagged APOBEC3G was a kind gift from Dr. Yasumasa Iwatani (National Hospital Organization Nagoya Medical Center, Nagoya, Japan) [19]. The Vif expression plasmid was obtained from Dr. Klaus Strebel (National Institutes of Health, Bethesda, MD, United States of America) [20], through Dr. Yasumasa Iwatani. The N-terminally SAMHD1n-fused APOBEC3G expression plasmid (SA3G) was generated as follows. The SAMHD1n-*Sal*I sequence was produced by PCR with the SAMHD1 F primer and the *Sal*I sequence-containing reverse primer 5'-CCCGTCGACATTAATTACCTTCAT-3', and cloned into the pCR 2.1 TOPO-vector (Invitrogen). The SalI-APOBEC3G-Myc plasmid was generated by introducing a *Sal*I sequence in frame at the 5' side of the start codon of the APOBEC3G-Myc expression plasmid with the *Sal*I sequence-containing forward primer, 5'-CTGCAGAATGTCGACATGAAGCCTCACTT -3', and a reverse primer, 5'-AGGCTTCATGTCGACATTCTGCAGATATCC-3'. The SAMHD1n-SalI plasmid was digested with the *Eco*RI and *Sal*I restriction enzymes. The SalI-APOBEC3G-Myc plasmid was digested with the *Sal*I and *Hind*III restriction enzymes. The Myc-tagged APOBEC3G expression plasmid was digested with the *Eco*RI and *Hind*III restriction enzymes and used as the vector. The *Eco*RI/*Sal*I-digested SAMHD1n fragment, the *Sal*I/*Hind*III-digested APOBEC3G fragment, and the *Eco*RI/*Hind*III-digested vector fragment were ligated.

All plasmids described above are driven by the CMV promoter. The nucleotide sequences of the plasmid DNAs constructed in this study were confirmed by sequencing (Applied Biosystems).

Transfection. 1x10^6 cells per 6cm culture-dish was seeded, and incubated at 37 °C in a 5% CO_2 incubator for 24 hrs. Two μg of plasmid DNA were mixed with 10 μl of FuGENE HD transfection reagent (Promega), in 100 μl of D-MEM medium without FBS and antibiotics. The transfection mixture was added to the cell supernatant.

SDS-PAGE and western blotting analysis. A 10 mM MG132 (Sigma) stock solution was prepared in dimethyl sulfoxide. At 24 hrs after transfection, the cell culture medium was replaced with fresh medium, and MG132 was added to a 5 μM final concentration. Cell lysates were prepared 24 hrs after with 1x sample buffer (10% glycerol, 1.5% SDS, 0.005% bromophenol blue, 50 mM Tris/HCl, pH 6.8), and equal quantities of total protein from each sample were fractionated by sodium dodecyl sulfate polyacrylamide gel electrophoresis (SDS-PAGE).

For western blot (WB) analyses, the proteins were transferred to a PVDF membrane (Millipore) in a wet blotter (Bio-Rad). The membranes were incubated with the corresponding primary antibodies overnight at 4 °C, and then incubated with HRP-conjugated anti-mouse IgG (Bio-Rad) or with protein G (Bio-Rad) for 1 hr at 4 °C. The primary antibody-bound proteins were visualized by enhanced chemiluminescence reagents (Bio-Rad). Immunoblotting images were captured using Fluor Chem Imaging System (IS-8800, Alpha Innotech). The relative intensity levels of each protein compared to β-actin were calculated with the equation, protein intensity/β-actin protein intensity by using Alpha Ease software.

Primary antibodies. Monoclonal antibodies against β-actin (Santa Cruz Biotechnology), HA (COVANCE), GFP (Nacalai Tesque), and Myc (Cell Signaling) were used. The anti-Vif antibody was obtained through the AIDS Research and Reference Reagent Program, NIAID, NIH, from Dr. Michael H. Malim [21,22]. Polyclonal antibody against human SAMHD1 (residues 88-337) was purchased from Proteintech (12586-1-AP).

Results

The SAMHD1 C-terminal HD domain-containing region is degraded in the proteasome, and the N-terminal SAM domain-containing region inhibits the degradation. THP-1 monocyte and U937 monocyte cells express and do not express endogenous SAMHD1 protein, respectively. However, the transduction of U937 cells with SAMHD1, followed by the PMA-induced differentiation dramatically restricts the HIV-1 infection similar extent to the PMA-differentiated THP-1 cells [6,9,15,23]. Why SAMHD1 becomes functional as an anti-HIV-1 factor after the PMA-induced differentiation in monocyte cells? To address this query, Lahouassa *et al.* showed that the expression of exogenous SAMHD1 protein was elevated after the PMA-induced differentiation in U937 cells [13]. This led us to speculate that the SAMHD1 protein level may be regulated at certain stage. Thus, we compared the endogenous SAMHD1 protein expression in THP-1 cells treated or untreated with the PMA stimulation. As shown in Figure 1A, the

SAMHD1 protein level was significantly enhanced by PMA stimulation in THP-1 cells. To know if these protein expression levels reflect a quantitative difference of SAMHD1 mRNA before and after the PMA stimulation, we performed the real-time PCR by using specific primers for SAMHD1 on total RNAs extracted from THP-1 cells treated with different PMA quantity (0, 10, 50, and 500 ng/mL). To our surprise, there was no difference in SAMHD1 mRNA level before and after the stimulation, regardless of increased quantity of the PMA (Fig. 1B). There are two possible ways to regulate protein abundance: post-transcriptional control of transcripts and post-translational control of protein. However, in many cases, protein abundance is post-translationally regulated by proteasomal degradation. In fact, the HD region contains many putative ubiquitination sites, as determined with the CKSAAP_UbSite program (data not shown). Thus, it is highly speculated that endogenous SAMHD1 protein expression was post-translationally regulated in THP-1 cells.

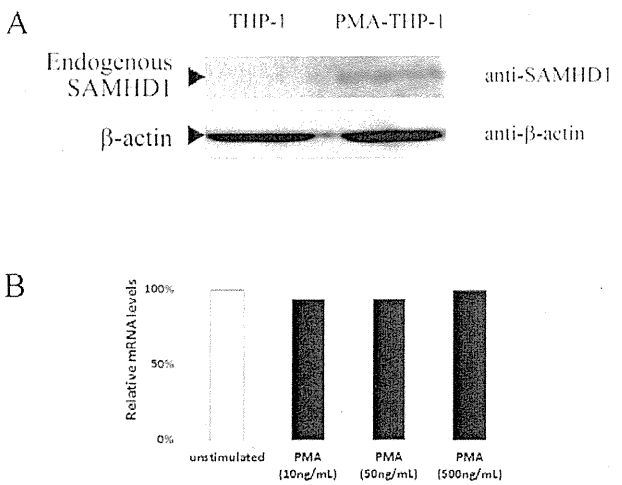

Figure 1. The SAMHD1 protein is post-translationally-regulated. (A) The endogenous SAMHD1 protein expression was analyzed in undifferentiated THP-1 and PMA-differentiated THP-1 cells. THP-1 cells were stimulated with 500ng/mL PMA for overnight. A WB analysis with a SAMHD1-specific antibody was performed. β-actin was detected as a loading control. (B) Real-time PCR for quantitation of SAMHD1 mRNA with specific primers were performed on THP-1 cells stimulated with different quantity of PMA. Relative quantities of SAMHD1 mRNA to GAPDH mRNA are indicated. Data are representative of similar results from two independent experiments.

We next wanted to identify which domain is responsible for the post-translational regulation of SAMHD1. We generated the C-terminally HA-tagged full-length SAMHD1 (1-626 aa), the N-terminal SAM domain-containing aa 1-119 region (SAMHD1n), and the C-terminal HD domain-containing aa 120-626 region (SAMHD1c) expression plasmids (Fig. 2A). Each plasmid was transfected into U937 cells and the cells were PMA-differentiated. As in undifferentiated THP-1 cells, none of the proteins were detected in undifferentiated U937 cells (Fig. 2B lane 1, 3, and 5). In contrary, all the proteins were expressed upon the PMA-induced differentiation, and the expression levels of the full-length SAMHD1 and SAMHD1n proteins were much higher than that of the SAMHD1c protein in PMA-differentiated U937 cells (Fig.2B, lane 2, 4, and 6), leading us to speculate that the SAMHD1n stabilizes the SAMHD1 protein in differentiated U937 cells. However, it may simply reflect the PMA stimulation-induced protein expression from CMV promoter [24]. We had previously searched for various cell lines in which SAMHD1 restricts HIV-1 infection without the PMA stimulation and, as a result, we found TE671 rhabdomyosarcoma cells moderately restricted the infection by transiently expressed SAMHD1 (manuscript in press). Of note, transiently expressed SAMHD1-mediated HIV-1 infection restriction was not observed in HeLa, H292, C33A, and NP2 (manuscript in press). Thus, in this study, we transfected each plasmid into TE671 cells and HeLa cells, the cells in which SAMHD1 does and does not restrict the HIV-1 vector infection, respectively, and the cells were treated with the proteasome inhibitor, MG132. As in PMA-differentiated U937 macrophage cells, the SAMHD1c protein was barely detected in TE671 cells and in HeLa cells, but the MG132 treatment significantly enhanced the protein abundances (Fig. 2C, lane 5 versus lane 6, and Fig. 3, lane 5 versus lane 6). These results indicated that the SAMHD1c protein is degraded by the proteasome. On the other hand, the amounts of the full-length SAMHD1 and SAMHD1n proteins were much higher than that of the SAMHD1c protein in TE671 cells (Fig.2C lane 1, 3, and 5), indicating that the SAMHD1n protects the full-length SAMHD1 protein from proteasomal degradation induced by SAMHD1c in TE671 cells. These former two protein expression levels are not significantly affected by the MG132 treatment (Fig. 2C lane 1 versus 2, and lane 3 versus 4), In contrary to that observed in TE671 cells, the amount of full-length protein was much lower than SAMHD1n protein in HeLa cells (Fig. 3 lane 1 versus 3), indicating that the SAMHD1n-mediated full-length SAMHD1 protein stabilization occurs more efficiently in TE671 cells than in HeLa cells. Moreover, the expression of full-length SAMHD1 was much higher than the SAMHD1n protein in U937 macrophage cells compare to that observed in TE671 cells (Fig. 2B lane 2 versus 4 and Fig.2C lane 1 versus 3). Thus, we speculate that the full-length SAMHD1

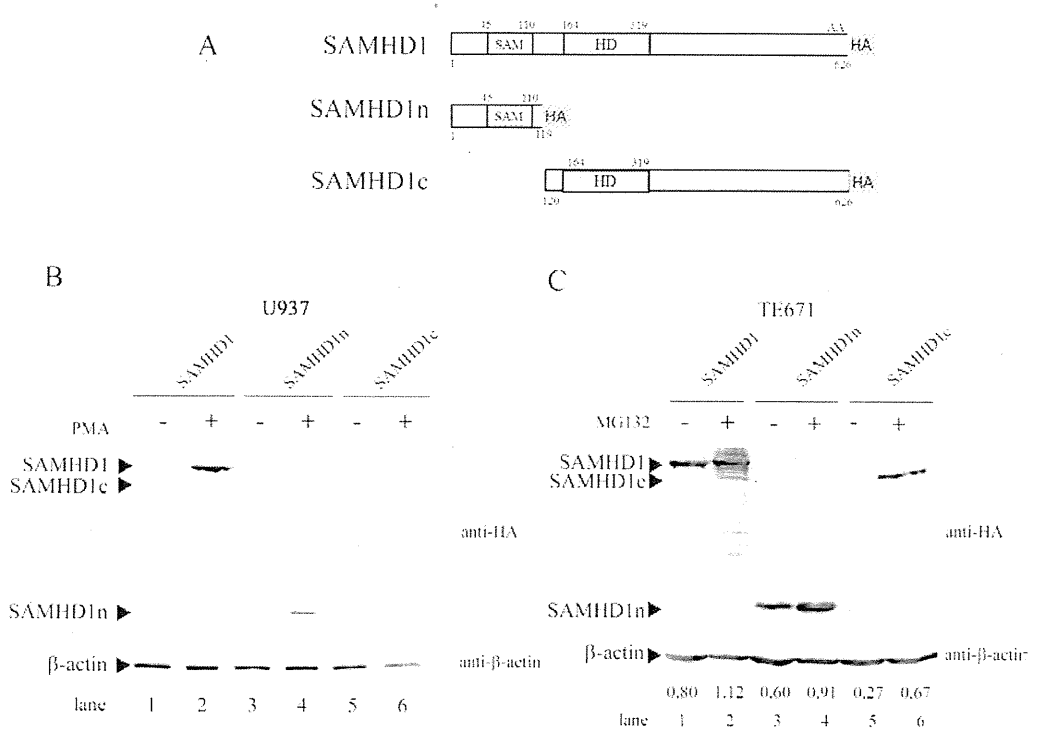

Figure 2. The SAMHD1c protein is degraded in the proteasome, and the SAMHD1n inhibits the degradation. (A) Schematic representations of SAMHD1 and its truncated mutants are indicated. SAMHD1 consists of the sterile-α motif (SAM) domain (aa 45-110) and the hydrolysis (HD) domain (aa 164-319). The SAMHD1n deletion mutant contains amino acid residues 1-119. The SAMHD1c mutant contains amino acid residues 120-626. Each plasmid encodes a C-terminally HA-tagged protein. Vectors encoding SAMHD1(1-626 aa), SAMHD1n (1-119 aa), and SAMHD1c (120-626 aa) were transfected into (B) U937 cells, followed by PMA untreatment or treatment for overnight, and into (C) TE671 cells, followed by MG132 untreatement or treatement for overnight. The samples were analyzed by WB, using anti-HA and anti-β-actin antibodies, in which β-actin was used as a loading control (B and C). Relative levels of each protein compared to β-actin are shown above the lane numbers (C). Data are representative of similar results from two independent experiments.

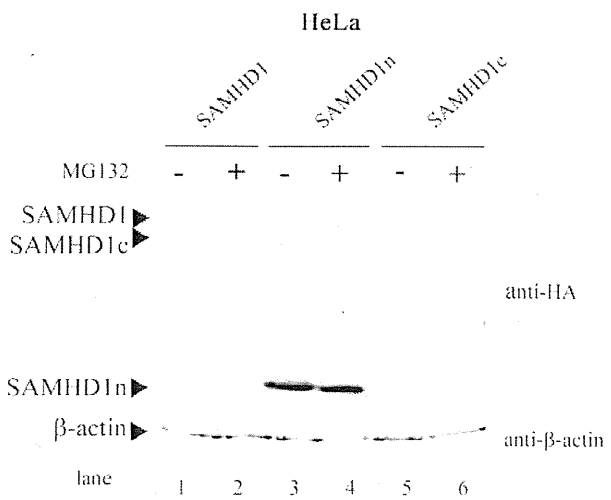

Figure 3. HeLa cells were untreated or treated with MG132 for overnight, followed by SDS-PAGE and WB. Each sample was analyzed with anti-HA and anti-β-actin antibodies. Data is a representative of similar results from two independent experiments.

protein stability may correlate with SAMHD1-mediated HIV-1 vector infection restriction. Overall, these results suggested that the SAMHD1n protects the SAMHD1 protein from the SAMHD1c -mediated proteasome degradation.

The SAMHD1 C-terminal region leads to the proteasome-dependent degradation of a heterologous protein. To assess the involvement of the SAMHD1c (120-626 aa) in the protein degradation, we constructed an expression plasmid encoding the C-terminally SAMHD1c-fused EGFP protein (GFP-HD) (Fig. 4A), and compared its expression with that of the control EGFP protein (GFP) in TE671 cells. As shown in Fig. 4B, the amount of the GFP-HD protein was increased by MG132 treatment, while the MG132 treatment did not significantly affect the GFP protein abundance. Our results clearly demonstrated that the SAMHD1c region has the ability to lead not only SAMHD1 but also a heterologous protein into proteasome-dependent degradation.

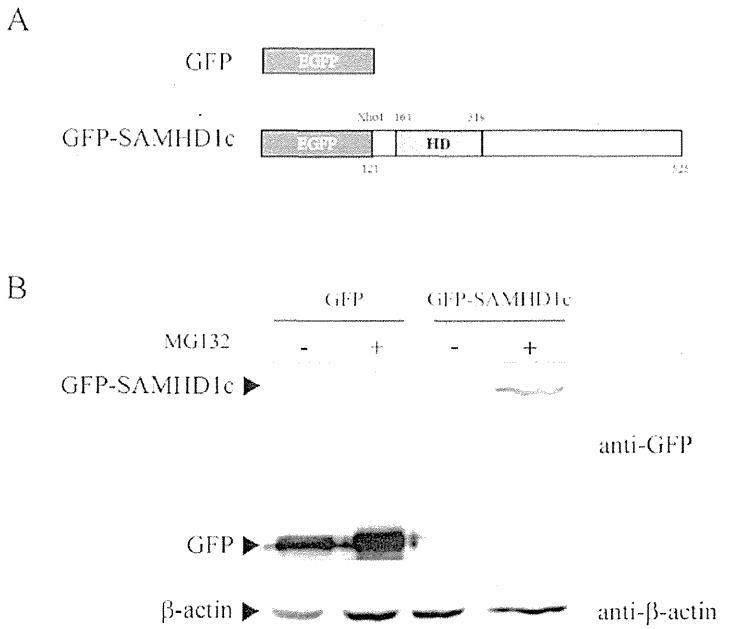

Figure 4. The SAMHD1c leads to proteasome-dependent degradation of a heterologous protein. (A) Schematic representations of GFP and C-terminally SAMHD1c fused GFP proteins are indicated. GFP and SAMHD1c were fused at the *Xho*I site. (B) GFP and GFP-SAMHD1c were transfected into TE671 cells. After 24 hrs of culture, the transfected cells were treated with MG132, and then further cultured for 24 hrs. Whole cell lysates were collected, fractionated by SDS-PAGE and analyzed by WB. The expression of the GFP and GFP-SAMHD1c proteins was analyzed with an anti-GFP antibody. *β*-actin was used as a loading control. Data are representative of similar results from two independent experiments.

The SAMHD1 N-terminal region protects full-length SAMHD1 from protesome-dependent degradation. To assess the role of the SAMHD1n in protein stabilization, we constructed an expression plasmid encoding an N-terminally SAMHD1n-fused, C-terminally Myc-tagged APOBEC3G protein (SA3G) (Fig. 5A). Human APOBEC3G (A3G) is degraded in the proteasome by the SIV or HIV-1 accessory protein, Vif [25,26]. The SA3G and A3G expression plasmids were co-transfected together with the Vif or control pcDNA3.1 expression plasmid into TE671 cells. As shown in Fig. 5B, similar levels of the SA3G and A3G proteins were detected without Vif. The Vif co-expression decreased the A3G protein expression (28-fold), while, the SA3G protein was slightly but steadily resistant to the Vif-mediated protesomal degradation (8-fold), indicating that the SAMHD1n can protect the heterologous A3G protein from proteasomal degradation in TE671 cells.

The SAMHD1 N-terminal region is critical for SAMHD1 stabilization in differentiated U937 cells. To know if the SAMHD1n-mediated protein stabilization is correlated to cell-type specific HIV-1 infection restriction ability of SAMHD1, the same experiment was performed on U937 cells, followed by PMA treatment. As in TE671 cells, the addition of Vif dramatically reduced the amount of the A3G protein (70-fold), while that of the SA3G protein was hardly affected (3-fold), indicating that SA3G was highly resistant to Vif-mediated proteasomal degradation in U937 cells (Fig. 5C). Although the SAMHD1n protected the A3G protein from Vif-mediated proteasomal degradation in TE671 cells, Vif still reduced the amount of the SA3G protein significantly in this cell line. Thus, these results suggested that the ability of the SAMHD1n to confer resistance to proteasome-dependent degradation was more prominent in U937 cells than in TE671 cells.

Trans-expression of SAM mutant protein does not affect SAMHD1 protein stability.

In addition, we tested if the *trans*-expressed SAMHD1n can rescue protein from the degradation. SAMHD1n expression plasmid was transfected into TE671 cells, together with the full-length SAMHD1 or SAMHD1c expression plasmid. As a result, neither the SAMHD1 nor SAMHD1c protein abundance was elevated by the trans-expression of

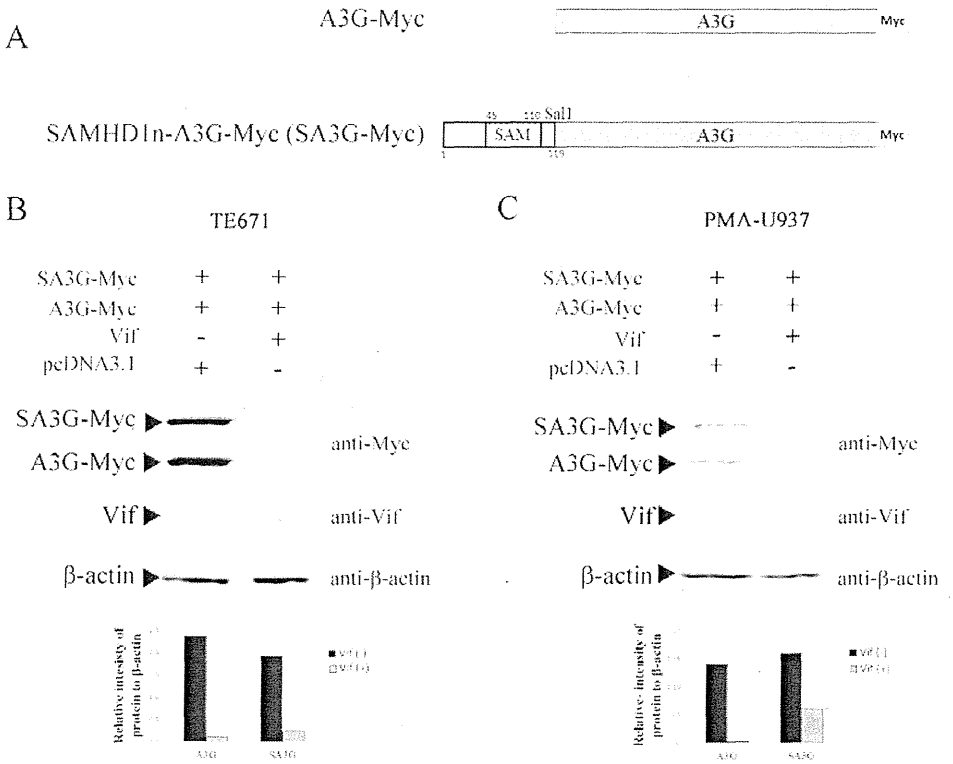

Figure 5. The SAMHD1n can protect a heterologous protein from proteasome-dependent degradation in TE671 and PMA-differentiated U937 macrophage cells. (A) Schematic representations of the A3G and N-terminally SAMHD1n-fused A3G (SA3G) proteins are indicated. SAMHD1n and A3G were fused at the *SalI* site. Each plasmid encodes a C-terminally Myc-tagged protein. (B) TE671 cells and (C) U937 cells were co-transfected with A3G and SA3G, together with pcDNA3.1 or Vif. U937 cells were treated with PMA after the transfection. The expression of the A3G and SA3G proteins was analyzed by WB, using the anti-Myc antibody. β-actin was used as a loading control and relative levels of each protein compared to β-actin are shown. Data are representative of similar results from two independent experiments.

SAMHD1n protein (Fig. 6), indicating that only the *cis*-linked SAMHD1n can protect the full-length SAMHD1 from degradation.

Discussion

Our study is the first report showing that the HD domain-containing C-terminal region of SAMHD1 is responsible for the proteasome-dependent degradation of SAMHD1 in the absence of Vpx, whereas the SAM domain-containing N-terminal region is critical for the stability of the full-length SAMHD1 protein. SAMHD1 can restrict HIV-1 vector infection in PMA-differentiated U937 macrophage and TE671 rhabdomyosarcoma cells, but not in HeLa cells. The SAMHD1n-mediated stabilization of the SAMHD1 protein occurs more efficiently in differentiated U937 cells than in TE671 cells, correlated to the degree of restriction of these cells. Interestingly, while we were preparing this manuscript, White *et al.* and Cribier *et al.* showed that the phos-

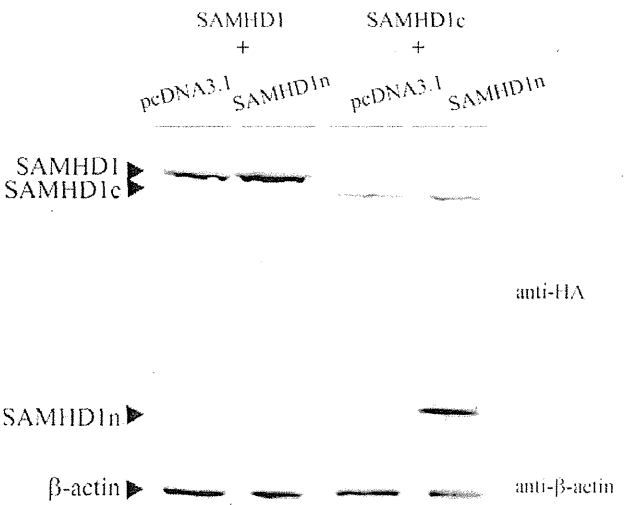

Figure 6. Trans expression of SAMHD1n mutant protein does not affect SAMHD1 protein stability. TE671 cells were transfected with a vector encoding the full-length SAMHD1 (left panel) or the SAMHD1c mutant (right panel) protein, together with pcDNA3.1 or the SAMHD1n mutant. Cell lysates from the transfected cells were analyzed by WB. Data are representative of similar results from two independent experiments.

phorylation of SAMHD1 determines the cell-type specific restriction of HIV-1 infection by SAMHD1 [27,28]. They proposed that the phosphorylation of SAMHD1 C-terminal at T592 aa regulates the retroviral restriction ability of SAMHD1. The close relationship between phosphorylation and ubiquitination has been well understood [29]. It is highly speculated that the ubiquitination of the SAMHD1c is also regulated by the phosphorylation of this region. Nevertheless, our study suggests that the stabilization of SAMHD1 by the SAMHD1n contributes to its restriction of HIV-1 infection.

Previous report has shown that N-terminal region-deleted SAMHD1 protein (112-626 aa) could still restrict HIV-1 vector infection in PMA-differentiated U937 cells [15], suggesting that the SAM domain containing N-terminal region is dispensable for the HIV-1 restrictive function of SAMHD1. However, it is still possible that the SAM domain participates in the infection restriction, since a SAM domain (45-110)-deleted SAMHD1 mutant protein reportedly fails to restrict HIV-1 infection in PMA-differentiated U937 cells, and its abundance is lower than that of the wild type SAMHD1 [15]. Several reports have shown that the amounts of N-terminally truncated SAMHD1 proteins are lower than that of the full-length protein [9,10,11,15,23]. In addition, recent report revealed that the SAMHD1 N-terminal region (1-118) is necessary to maximize the dGTP triphosphatase and nuclease activities, and indispensable for nucleic acid and viral genome binding activities of SAMHD1 [14]. Together, these reports suggested that the SAM domain is necessary for the SAMHD1-mediated restriction of HIV-1 infection and protein stability.

Notably, the SA3G protein was remarkably resistant to the Vif-induced degradation in differentiated U937 cells. The tertiary structure of SA3G is considered to have minor or no effect to the A3G interaction with Vif by the SAMHD1n fusion, because the amount of the SA3G protein was significantly reduced by Vif in TE671 cells. To further support the involvement of the SAM domain in the protein protection from proteasome-dependent degradation, Park *et al.* [30] reported an interesting feature about the SAM domain of the tyrosine kinase-type A2 receptor (EPHA2) protein: the group showed that the SAM domain of the EPHA2 protein plays a critical role in its stability, by modulating the proteasome-dependent process. The SAMHD1 SAM domain shares 40% similarity and 16% identity with that of EPHA2 (Phyre2 program). The SAM domain is responsible for protein-protein or protein-RNA interactions [31]. Therefore, an interaction between the SAMHD1n and an unknown cellular factor may stabilize the SAMHD1 protein.

Vpx at its N-terminal region forms a complex with SAMHD1 C-terminal region (606-626 aa) and loads it to the $CRL4^{DCAF1}$ ubiquitin E3 ligase, followed by proteasomal degradation[11]. However, we have shown that the SAMHD1c contains a motif that leads SAMHD1 into proteasome-dependent degradation, in the absence of Vpx. The SAMHD1 protein may be stabilized by an intramolecular interaction between the SAMHD1n and SAMHD1c regions. Vpx may compete with the SAMHD1n, and induce the degradation of the full-length SAMHD1 protein. Identifying the relationship between these core domain containing regions and the Vpx is our next target of interest in parallel with disclosing the contribution of SAMHD1c phosphorylation to the full-length SAMHD1 stability.

In summary, the HD domain-containing C-terminal region leads the SAMHD1 protein to proteasomal degradation. The SAM domain-containing N-terminal region stabilizes the SAMHD1 protein efficiently in differentiated U937 cells and in TE671 cells, in which SAMHD1-mediated HIV-1 infection restrictions were observed, suggesting that the SAM-mediated stabilization of the SAMHD1 protein is important for its anti-virus activity. Further studies are required to understand the mechanism by which the SAMHD1n stabilizes the SAMHD1 protein.

Acknowledgements

We thank a member of Division of Cytokine Signaling laboratory for helpful discussion. We are grateful to Fumiyo Tsujita and Yuri Kobayashi for their continuous assistance. We are grateful to Drs. Yasumasa Iwatani and Klaus Strebel for providing the plasmids encoding APOBEC3G and Vif. We thank Michael Malim for the anti-Vif antibody, through the AIDS Research Reference Reagent Program, NIAID, NIH, USA. We also thank Dr. Mana Miyakoda for technical advice. This work was supported by Grants-in-Aid from the Ministry of Education, Culture, Sports, Science and Technology of Japan and by the Global Center of Excellence Program at Nagasaki University.

References

[1] N. Li, W. Zhang, X. Cao, Identification of human homologue of mouse IFN-gamma induced protein from human dendritic cells, Immunol Lett 74 (2000) 221-224.

[2] W. Liao, Z. Bao, C. Cheng, *et al.*, Dendritic cell-derived interferon-gamma-induced protein mediates tumor necrosis factor-alpha stimulation of human lung fibroblasts, Proteomics 8 (2008) 2640-2650.

[3] C. St Gelais, S. de Silva, S.M. Amie, *et al.*, Hollenbaugh, B. Kim, L. Wu, SAMHD1 restricts HIV-1 infection in dendritic cells (DCs) by dNTP depletion, but its expression in DCs and primary CD4 T-lymphocytes cannot be upregulated by interferons, Retrovirology 9 (2012) 105.

[4] L. Dragin, L.A. Nguyen, H. Lahouassa, *et al.*, Interferon block to HIV-1 transduction in macrophages despite SAMHD1 degradation and high deoxynucleoside triphosphates supply, Retrovirology 10 (2013) 30.

[5] G.I. Rice, J. Bond, A. Asipu, *et al.*, Mutations involved in Aicardi-Goutières syndrome implicate SAMHD1 as regulator of the innate immune response, Nat Genet 41 (2009) 829-832.

[6] N. Laguette, B. Sobhian, N. Casartelli, *et al.*, SAMHD1 is the dendritic- and myeloid-cell-specific HIV-1 restriction factor counteracted by Vpx, Nature 474 (2011) 654-657.

[7] K. Hrecka, C. Hao, M. Gierszewska, *et al.*, Vpx relieves inhibition of HIV-1 infection of macrophages mediated by the SAMHD1 protein, Nature 474 (2011) 658-661.

[8] H.M. Baldauf, X. Pan, E. Erikson, *et al.*, SAMHD1 restricts HIV-1 infection in resting CD4(+) T cells, Nat Med 18 (2012) 1682-1687.

[9] A. Brandariz-Nuñez, J.C. Valle-Casuso, *et al.*, Role of SAMHD1 nuclear localization in restriction of HIV-1 and SIVmac, Retrovirology 9 (2012) 49.

[10] H. Hofmann, E.C. Logue, N. Bloch, *et al.*, The Vpx lentiviral accessory protein targets SAMHD1 for degradation in the nucleus, J Virol 86 (2012) 12552-12560.

[11] J. Ahn, C. Hao, J. Yan, *et al.*, HIV/simian immunodeficiency virus (SIV) accessory virulence factor Vpx loads the host cell restriction factor SAMHD1 onto the E3 ubiquitin ligase complex CRL4DCAF1, J Biol Chem 287 (2012) 12550-12558.

[12] D.C. Goldstone, V. Ennis-Adeniran, J.J. Hedden, *et al.*, HIV-1 restriction factor SAMHD1 is a deoxynucleoside triphosphate triphosphohydrolase, Nature 480 (2011) 379-382.

[13] H. Lahouassa, W. Daddacha, H. Hofmann, *et al.*, SAMHD1 restricts the replication of human immunodeficiency virus type 1 by depleting the intracellular pool of deoxynucleoside triphosphates, Nat Immunol 13 (2012) 223-228.

[14] N. Beloglazova, R. Flick, A. Tchigvintsev, *et al.*, Nuclease Activity of the Human SAMHD1 Protein Implicated in the Aicardi-Goutieres Syndrome and HIV-1 Restriction, J Biol Chem (2013).

[15] T.E. White, A. Brandariz-Nuñez, J. Carlos Valle-Casuso, *et al.*, Contribution of SAM and HD domains to retroviral restriction mediated by human SAMHD1, Virology 436 (2013) 81-90.

[16] B. Descours, A. Cribier, C. Chable-Bessia, *et al.*, SAMHD1 restricts HIV-1 reverse transcription in quiescent CD4(+) T-cells, Retrovirology 9 (2012) 87.

[17] M.N. Lee, M. Roy, S.E. Ong, *et al.*, Identification of regulators of the innate immune response to cytosolic DNA and retroviral infection by an integrative approach, Nat Immunol 14 (2013) 179-185.

[18] J. Korczeniewska, B.J. Barnes, The COP9 Signalosome Interacts with and Regulates Interferon Regulatory Factor 5 Protein Stability, Mol Cell Biol 33 (2013) 1124-1138.

[19] Y. Iwatani, D.S. Chan, L. Liu, *et al.*, HIV-1 Vif-mediated ubiquitination/degradation of APOBEC3G involves four critical lysine residues in its C-terminal domain, Proc Natl Acad Sci U S A 106 (2009) 19539-19544.

[20] K.L. Nguyen, M. Llano, H. Akari, *et al.*, Codon optimization of the HIV-1 vpu and vif genes stabilizes their mRNA and allows for highly efficient Rev-independent expression, Virology 319 (2004) 163-175.

[21] J.H. Simon, T.E. Southerling, J.C. Peterson, B.E. Meyer, M.H. Malim, Complementation of vif-defective human immunodeficiency virus type 1 by primate, but not nonprimate, lentivirus vif genes, J Virol 69 (1995) 4166-4172.

[22] J.H. Simon, R.A. Fouchier, T.E. Southerling, *et al.*, The Vif and Gag proteins of human immunodeficiency virus type 1 colocalize in infected human T cells, J Virol 71 (1997) 5259-5267.

[23] J. Yan, S. Kaur, M. Delucia, *et al.*, Tetramerization of SAMHD1 is required for biological activity and inhibition of HIV infection, J Biol Chem (2013).

[24] P. Ruybal, M.J. Gravisaco, V. Barcala, *et al.*, Transgene expression enhancement in T-lymphoma cell lines, Int Immunopharmacol 5 (2005) 1685-1692.

[25] S. Jäger, D.Y. Kim, J.F. Hultquist, *et al.*, Vif hijacks CBF-β to degrade APOBEC3G and promote HIV-1 infection, Nature 481 (2012) 371-375.

[26] X. Yu, Y. Yu, B. Liu, *et al.*, Induction of APOBEC3G ubiquitination and degradation by an HIV-1 Vif-Cul5-SCF complex, Science 302 (2003) 1056-1060.

[27] T.E. White, A. Brandariz-Nuñez, J.C. Valle-Casuso, *et al.*, The Retroviral Restriction Ability of SAMHD1, but Not Its Deoxynucleotide Triphosphohydrolase Activity, Is Regulated by Phosphorylation, Cell Host Microbe 13 (2013) 441-451.

[28] A. Cribier, B. Descours, A.L. Valadão, *et al.*, Phosphorylation of SAMHD1 by Cyclin A2/CDK1 Regulates Its Restriction Activity toward HIV-1, Cell Rep (2013).

[29] T. Hunter, The age of crosstalk: phosphorylation, ubiquitination, and beyond, Mol Cell 28 (2007) 730-738.

[30] J.E. Park, A.I. Son, R. Hua, *et al.*, Human cataract mutations in EPHA2 SAM domain alter receptor stability and function, PLoS One 7 (2012) e36564.

[31] F. Qiao, J.U. Bowie, The many faces of SAM, Sci STKE 2005 (2005) re7.